https://doi.org/10.5194/egusphere-2023-1302
Preprint. Discussion started: 1 August 2023

Lahar events in the last 2,000 years from Vesuvius eruptions. Part 1: Distribution and impact on densely-inhabited territory estimated from field data analysis

Mauro A. Di Vito (1,*), Ilaria Rucco (2), Sandro de Vita (1), Domenico M. Doronzo (1), Marina Bisson (3), Mattia de' Michieli Vitturi (3), Mauro Rosi (4), Laura Sandri (5), Giovanni Zanchetta (4), Elena Zanella (6), Antonio Costa (5)

(1) Istituto Nazionale di Geofisica e Vulcanologia - Sezione di Napoli Osservatorio Vesuviano, Napoli, Italy

(2) Heriot-Watt University, School of Engineering and Physical Sciences, Edinburgh, United Kingdom

(3) Istituto Nazionale di Geofisica e Vulcanologia - Sezione di Pisa, Pisa Italy

(4) Università di Pisa, Dipartimento di Scienze della Terra, Pisa, Italy

(5) Istituto Nazionale di Geofisica e Vulcanologia - Sezione di Bologna, Bologna, Italy

(6) Università di Torino, Dipartimento di Scienze della Terra, Torino, Italy

*Corresponding author: Mauro A. Di Vito (mauro.divito@ingv.it)

Abstract

Lahars represent some of the most dangerous phenomena in volcanic areas for their destructive power, causing dramatic changes in the landscape with no premonitory signs and impacting on population and infrastructures. In this regard, the Campanian Plain turns out to be very prone to the development of these phenomena, since the slopes of the Somma-Vesuvius and Campi Flegrei volcanoes, along with the Apennine reliefs are mantled by pyroclastic deposits that can be easily remobilised, especially after intense and/or prolonged rainfall.

This study focuses on the analysis of the pyroclastic fall and flow deposits and of the syn- and post-eruptive lahar deposits related to two sub-Plinian eruptions of Vesuvius, 472 AD (Pollena) and 1631. To begin with, historical and field data from the existing literature and from hundreds of outcrops were collected and organized into a database, which was integrated with several new pieces of data.

https://doi.org/10.5194/egusphere-2023-1302
Preprint. Discussion started: 1 August 2023

In particular, stratigraphic, sedimentological (facies analysis and laboratory) and archaeological analyses were carried out, in addition to rock magnetic investigations and impact parameter calculations. The new data are mainly referred to the finding of ash beds in more distal areas, which was included into new isopach maps for the two sub-Plinian eruptions.

The results show that for both the eruptions the distribution of the primary deposits is wider than the one previously known. A consequence of these results is that a wider areal impact should be expected in terms of civil protection, as the sub-Plinian scenario is the reference one for a future large eruption of Vesuvius. Such distribution of the pyroclastic deposits directly affects the one of the lahar deposits, also because a significant remobilization took place during and after the studied eruptions which involved the distal phreatomagmatic ash. From these integrated analyses, it was possible to constrain the timing of the deposition and the kind of deposits remobilized (pyroclastic fall vs. flow), as well as was possible to calculate the velocities and dynamic pressures of the lahars, and ultimately infer the lahar transport and emplacement mechanisms.

The multidisciplinary approach adopted in this work shows how it is crucial to assess the impact of lahars in densely populated areas even at distances of several to tens of km from active volcanoes. This especially applies to large parts of the densely populated areas around Somma-Vesuvius up to the nearby Apennine valleys.

Keywords: Somma-Vesuvius; Apennine valleys; pyroclastic deposits; lahars; areal distribution; local impact.

1. Introduction

The emplacement of volcaniclastic mass flows, and the consequent damage along the flanks of active volcanoes and perivolcanic plains, represent a constant threat to inhabited areas and populations (e.g., Waitt et al., 1983; Lowe et al., 1986; Pierson, 1985; Newhall and Punongbayan, 1996). These

https://doi.org/10.5194/egusphere-2023-1302
Preprint. Discussion started: 1 August 2023

phenomena are triggered by various mechanisms, among which the most common are intense or prolonged atmospheric precipitations (Arguden and Rodolfo, 1990; Rodolfo and Arguden, 1991; Pareschi et al., 2000; Rodolfo, 2000; Scott et al., 2001; Vallance and Iverson, 2015). Such precipitations, especially during and/or immediately after the eruptions, cause the detachment of landslides that can evolve into lahars (e.g., White et al., 1997; Sheridan et al., 1999; Scott et al., 2001). The last century was affected by a significant number of highly-impacting lahar events associated to well-studied explosive volcanic eruptions worldwide, such as for example at Colima (Mexico) in 1913 (Rodriguez-Sedano et al., 2022), Nevado del Ruiz (Colombia) in 1985 (Voight, 1990), Ruapehu (New Zealand) in 2007 (Lube et al., 2012), and Merapi (Indonesia) in 2011 (Jenkins et al., 2015).

According to Rodolfo (2000), Sulpizio et al. (2006), and Vallance and Iverson (2015), volcaniclastic mass flows can be generated at variably long time-intervals, spanning from eruption to post-eruptive phases of tens to hundreds years. In case they are directly related to volcanic eruptions or are penecontemporaneous to them (i.e., during or shortly after the eruptive event), lahars are defined as syn-eruptive, and can represent an important hazard factor in the short to middle term for perivolcanic areas (Rodolfo, 2000; Sulpizio et al., 2006). On the other hand, in case they are unrelated to any eruption dynamics, so occurring during volcanic quiescence, they are defined as post- or inter-eruptive (Vallance and Iverson, 2015), and can represent a long-term hazard factor (e.g., Siebe et al., 1999; Pareschi et al., 2002; Zanchetta et al., 2004a, 2004b; Sulpizio et al., 2006). Usually, these latter are not accounted for in assessing volcanic hazard, although their study is important for long-term territorial planning.

In this sense, i.e. from the hazard assessment point of view, one of the priorities concerns the assessment of those areas potentially exposed to such a threat, taking into account the temporal recurrences of the phenomena (during days to months after an eruption, or years to decades after) and the physical features of the volcaniclastic mass flows (volume, thickness, velocity, dynamic pressure, concentration, and invasion areas).

https://doi.org/10.5194/egusphere-2023-1302
Preprint. Discussion started: 1 August 2023

A lot of the existing literature analyzed the hazard related with volcaniclastic mass flows on the flanks of active volcanoes, through the reconstruction of historical and prehistoric events (e.g., Scott, 1989; Scott et al., 1995; Vallance and Scott, 1997), by using empirical relationships or physical models (e.g., Macedonio and Pareschi, 1992; Costa, 1997; Iverson et al., 2000). However, the areas affected by these phenomena can be extended well beyond the boundaries of the volcanic complex, also including the surrounding plains and the downwind-lying mountainous areas, which are subjected to tephra fallout sometimes even at great distances from the volcano (e.g., Siebe et al., 1999; Pareschi et al., 2000, 2002; Zanchetta et al., 2004a, 2004b; Di Crescenzo and Santo, 2005). In these areas, volcaniclastic mass flows may cause victims and damages, even where considered safe or scarcely affected by other volcanic hazards.

In this paper, we present the results of a multidisciplinary study, including geomorphological, stratigraphic, sedimentological and rock magnetic investigations, as well as impact parameter calculations by reverse engineering from the deposits. These investigations followed several surveying campaigns carried out in natural exposures, archaeological excavations, and trenches dug specifically for this purpose in the plain surrounding the Vesuvius edifice and along the Apennine valleys (Fig. 1). One of the goals of the study is to show the presence of lahar deposits even in areas very far from both the Apennine hills and the valleys of Somma-Vesuvius, demonstrating the high mobility of these flows. Technically, the ones descending on the Apennine flanks should be termed as volcaniclastic debris flows; here we merge into an only one term, lahars, to indicate secondary mass flows strictly related to specific eruptions. The study of the past deposits has been useful for the understanding of the feeding drainage basins for different types of volcaniclastic mass flows, their extent and facies variations with distance from the source area, and their environmental impact. As already pointed out by Di Vito et al. (2013, 2019), in the past 4.5 ka repeated lahar and flooding episodes related to the main eruptions of Somma-Vesuvius and Campi Flegrei volcanoes strongly stroke the Campanian Plain and its human settlements, influencing their abandonment or evidencing attempts of resettlement. In particular, for the areas around Vesuvius, these phenomena included: i)

https://doi.org/10.5194/egusphere-2023-1302
Preprint. Discussion started: 1 August 2023

large volume and high energy lahars, originated from the volcanic edifice, which affected the volcanic apron; ii) large flooding phenomena affecting the Campanian plain; iii) lahars originated from the perivolcanic mountains that affected the Apennine valleys and invaded the areas of the plain at their mouth. The data and pieces of information described here were the basis for validating a new model for lahar transport (de' Michieli Vitturi et al., submitted), which was applied for assessing the related hazard at Vesuvius and Campanian Plain (Sandri et al., submitted).

The structure of the work consists of a geological, geomorphological, stratigraphic and sedimentological integrated study, a paleomagnetic and sediment-mechanic impact assessment calculation, and a comprehensive discussion on the lahar problem in the Campanian Plain.

2. Geological setting

The study area is part of the Campanian Plain, which includes the lowlands surrounding Mount Vesuvius volcano and the nearby Apennine ridges and valleys (Fig. 1). The orography of the area is characterized by three WNW-ESE trending mountain ridges that border eastward the plain, with an elevation ranging from 500 to 1600 m a.s.l., and slope angles from 30 to 60°. From north to south, the Avella-Partenio, Lauro-Visciano and Sarno-Quindici mountain ridges are separated by two depressions: the Avella-Baiano valley, in which the alluvial plain of the Clanio river occur, and the Lauro valley. Both are narrow valleys that widen toward north-west, among the cities of Cicciano, Nola and Palma Campania (Fig. 1). The reliefs are characterized by a high drainage density, associated with a poorly developed and torrential hydrographic network, which over time has favored the incision and dismantling of the pyroclastic cover on the ridges, and the development of numerous detrital conoids that connect with the main valley floor (Di Vito et al., 1998).

https://doi.org/10.5194/egusphere-2023-1302
Preprint. Discussion started: 1 August 2023

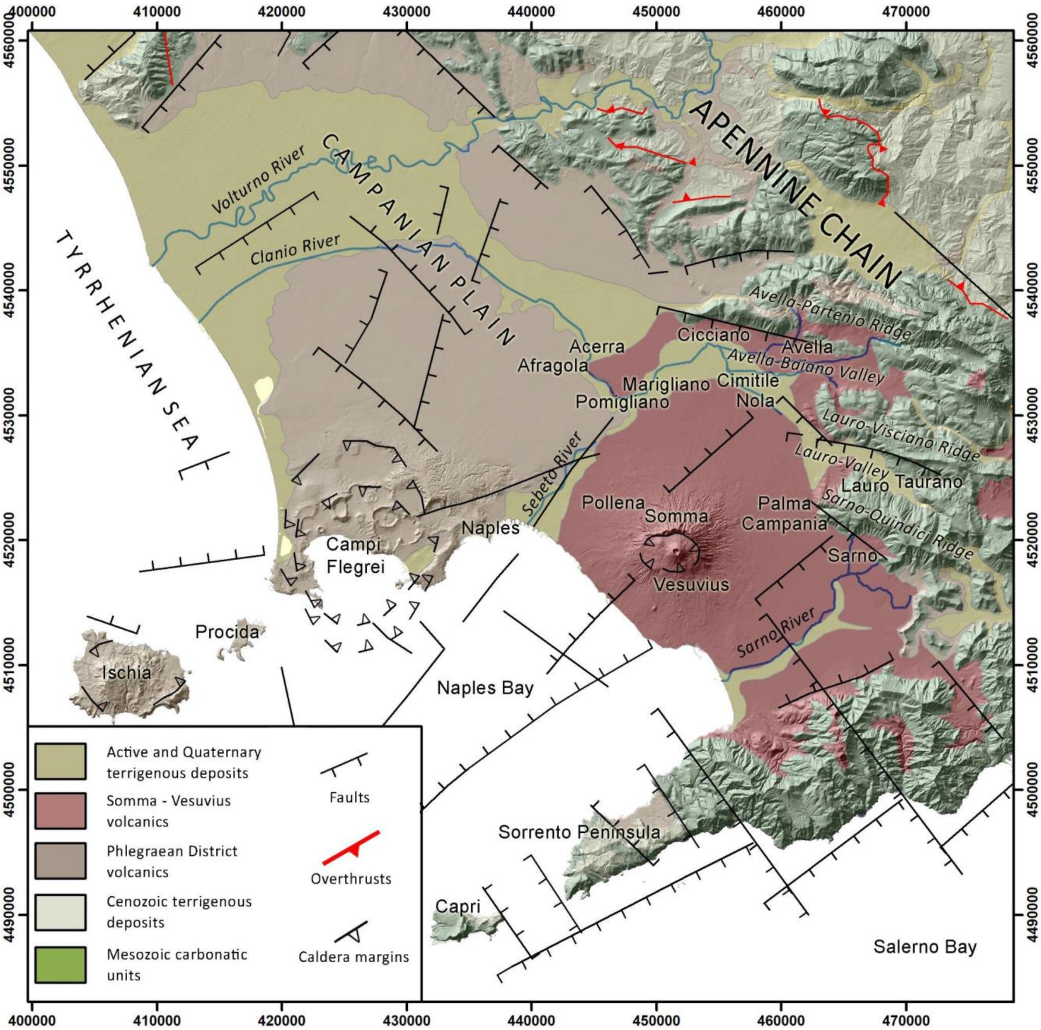

Fig. 1. Geological and structural sketch of the Campania Region on a Shaded Relief derived from TINITALY DEM. The coordinates are expressed in WGS 84 UTM N33 (modified after Orsi et al., 1996).

Mount Vesuvius is a composite central volcano with a well-developed radial drainage network, which feeds an extensive volcaniclastic apron that morphologically connects the edifice with the surrounding plain (Santacroce et al., 2003). It represents the active southern termination of the Plio-Quaternary volcanic chain that borders the eastern Tyrrhenian margin (Peccerillo, 2003). Volcanism in this margin is related to the extensional tectonic phases that accompanied the anticlockwise rotation

https://doi.org/10.5194/egusphere-2023-1302
Preprint. Discussion started: 1 August 2023

of the Italian peninsula, during the complex interaction between the Africa and Eurasian plates, which generated the Apennine thrust-and-fold belt (Ippolito et al., 1973; D'Argenio et al., 1973; Finetti and Morelli, 1974; Bartole, 1984; Piochi et al., 2004; Patacca and Scandone, 2007; Vitale and Ciarcia, 2018). The extension along the Tyrrhenian margin of the Apennine chain was accommodated by the activation of NW-SE normal faults and NE-SW normal to strike-slip transfer fault systems, which dismembered the chain in horst and graben structures, and allowed magmas to reach the surface and feed the volcanism (Mariani and Prato, 1988; Faccenna et al., 1994; Acocella and Funiciello, 2006). The Campanian Plain is one of these grabens that hosts the Neapolitan volcanic area. It is a NW-SE elongated structural depression, filled by a thick sequence of marine and continental sedimentary deposits, and volcanic-volcaniclastic successions that compensated its subsidence, leading to a complete emersion at around 39 ka (Brocchini et al., 2001; De Vivo et al., 2001; Santangelo et al., 2017). This graben is bordered toward NW, NE and SE by the Meso-Cenozoic carbonate and terrigenous successions of the Apennine chain, and is subdivided in minor NE-SW oriented horst-and-graben structures (Carrara et al., 1973; Finetti and Morelli, 1974; Fedi and Rapolla, 1987; Brancaccio et al., 1991). Neapolitan volcanoes lie on these second order structural highs (Marotta et al., 2022 and reference therein), and the products of their most powerful eruptions blanketed the Apennine reliefs and filled their valleys with several meter-thick cover of loose pyroclastic deposits, composed of pumice lapilli and ash layers separated by paleosoils (Pareschi et al., 2002; Bisson et al., 2007; Cinque and Robustelli, 2009).

In terms of drainage of the water, the pyroclastic cover has peculiar geotechnical characteristics, which enabled the development of lahars in the area. In particular, coarser pumice layers are characterized by interconnected inner voids that control water accumulation, instead soils and paleosoils by a high water retention capacity (Andosol-like soils), so that the differential behavior can regulate equilibrium among deposits stability vs. remobilization (Fiorillo and Wilson, 2004).

Regarding the volcanic activity of Vesuvius in the last 2,000 years, the largest eruptions after the 79 CE Plinian one were two sub-Plinian eruptions, the 472 CE Pollena and 1631 ones, but several other

https://doi.org/10.5194/egusphere-2023-1302
Preprint. Discussion started: 1 August 2023

effusive and explosive events frequently occurred in historical times. In the Campanian Plain, lahar deposits related to these two eruptions are quite abundant, also the sub-Plinian scenario is of interest for civil protection purposes, which is why in the present work we focus on these reference explosive eruptions. Throughout the work, a particular attention is put on distribution of the primary pyroclastic deposits and the related syn-eruptive lahars, which are mass flow events strictly related to specific eruptions, even if the condition is not necessarily that of an event contemporaneous to the eruption; those deposits are mainly composed by >90% fragments from the parental eruption (Sulpizio et al., 2006). The syn-eruptive feature is thus related to the involvement of pyroclastic deposits more than to the exact timing of emplacement, the latter being of the order of max a few years (before significant humification processes can occur).

3. Materials and methods

3.1. Evidence from historical sources

We collected data from historical sources, maps, documents, and newspapers to supplement the geological data, gathered directly or indirectly, for the definition of the areal distribution of the syn-eruptive and post-eruptive lahar deposits at Vesuvius and in the surrounding region. Such collection concerned the phenomena that took place starting from the sixteenth century CE to 2005. This time span has been chosen depending on data availability, and to show the high recurrence of events over time in the area. The data were collected and grouped not only by years but also by the municipal areas existing at those times. It should be noted that the distribution of the data can be affected by the different urbanization over time, and by the presence of damage to people, things, economic activities and settlements. In the absence of local instrumental meteorological series, corresponding to the analyzed period, we assumed that the phenomena of remobilization of the pyroclastic deposits, and the consequent generation of large alluvial events and volcaniclastic mass flows, coincided with extreme weather events often described and reported in the analyzed sources. The reports reach a

https://doi.org/10.5194/egusphere-2023-1302
Preprint. Discussion started: 1 August 2023

quite significant number, approximately 500, and concern 97 municipalities. The data were organized in a geospatial database, so that it was possible to define different areas affected by frequent syn-eruptive floods and lahars, concomitant/related with the sub-Plinian eruption of 1631, to be used as benchmark for the main geological analyses. With reference to the Pollena eruption, there are no historical sources for similar occurrences other than documents deriving from archaeological excavation activities (see next sections).

The municipalities with the highest number of reports are: Sarno (43), Salerno (32), Siano (26), Vietri sul Mare (22), Bracigliano (21), Nocera Inferiore (20), Maiori (19), Quindici (17) (Fig. 1). The events of greatest intensity, which affected more than five municipal territories at the same time, are 19; they likely were multiple soil-slip debris flows. Some of these occurrences result closely connected with the volcanic events of Vesuvius, such as those that occurred in 1631, 1823, 1910, 1949 and 1954, simultaneously or within months to a few years after the eruptions of 1631, 1822, 1906 and 1944. The absence of information in the Lauro and Avella-Baiano Valleys is likely due to the absence of detailed descriptions of alluvial events, or most likely to the position of the inhabited areas generally located on the hills thus far from the lower part of the valleys.

3.2. Field and archaeological investigations

We used a set of geological, stratigraphical, sedimentological, archaeological, and pedological information for the reconstruction of the type of events, their emplacement mechanisms, timing, and impact on pre-existing structures/environment. Such an approach enabled us to cross-check geological and archaeological evidence allowing us to accurately fix the age of events. Conversely, the presence of well-dated primary pyroclastic deposits can define the age of human traces otherwise not easily datable. Furthermore, the identification of the "primary" (fallout and pyroclastic current, along with the archeological findings) can give the absolute age (*ante* or *post quem*) of a given deposit. The definition of isochronic paleosurfaces can also contribute to the reconstruction of the paleo-

https://doi.org/10.5194/egusphere-2023-1302
Preprint. Discussion started: 1 August 2023

environments affected by the deposition, and of the variations that occurred during depositional processes. For this purpose, particular attention was paid to the basal contacts between the deposits. In some areas like Nola, the lahar deposits directly overlie the primary pyroclastic deposits (of Pollena or 1631 eruption), while in other cases some units or the whole primary deposits are missing (eroded) or lacking. Only the correlation with the nearby areas permitted to define whether the emplacement of the secondary deposits eroded partly or entirely the primary deposits, vice versa the absence was ‘‘simply’’ due to their distribution. The analysis of the internal structure marked by sharp changes in grain sizes, color, presence of erosive unconformities, or interposition of lenses of coarser material also permitted the identification of one or more flow units within the same individual deposit package. The macroscopic characteristics of the sequences permitted some inferences on the transport and depositional mechanisms, while the componentry analysis provided information of the source deposits that were remobilized. This brings to another important definition, that is syn- vs post-eruptive lahars, according to the definition of Sulpizio et al. (2006), which applies respectively soon after the eruption vs. years to centuries after the eruption ended. The macroscopic analysis allowed us to distinguish between the syn-eruptive deposits, which are defined by the occurrence of pyroclastic components with homogeneous lithology, similar to the primary deposits, and the post- (or inter-) eruptive deposits, characterized by evidence of depositional stasis, such as humified paleosurfaces, evidence of anthropic activity, or also through deposits that contain humified material and/or fragments of older eruptions following the progressive erosion within the feeding slopes and valleys. All these characteristics allowed the correlation between the various volcaniclastic units for the whole set of the studied sequences, marking the differences needed to hypothesize on the source and invasion areas.

We reviewed all the volcanological and archaeological data collected during the last 20 years from drill cores, outcrops, archaeological excavations, and from the existing literature, in collaboration with colleagues of the Archaeological Superintendence of Campania region. The preliminary collection and analysis of the existing data permitted to plan a hundred of new stratigraphic trenches

https://doi.org/10.5194/egusphere-2023-1302
Preprint. Discussion started: 1 August 2023

(Fig. 2), with the aim of collecting stratigraphic, stratimetric, sedimentological, lithological and chronological data on the sequences both of primary pyroclastic and secondary (lahar) deposits. Particular attention was paid to the primary pyroclastic deposits and to syn- and post-eruptive lahars, and to their geometric relations with the paleotopography and the preexisting anthropic structures.

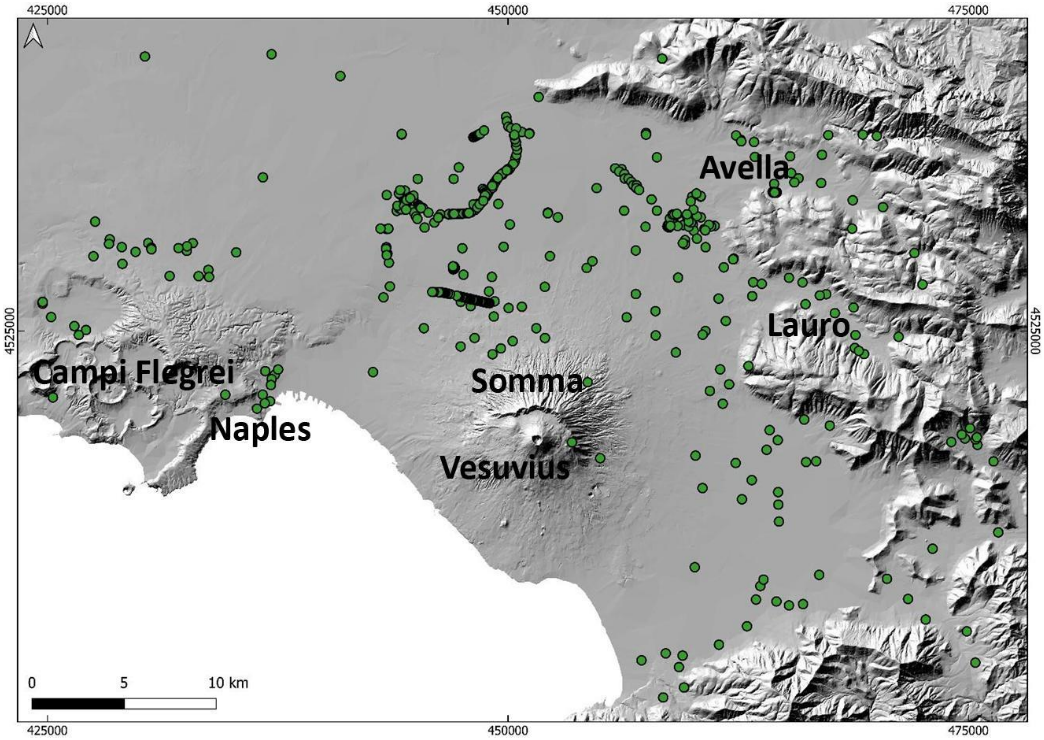

Fig. 2. Shaded relief of the studied area and location of all the sites where stratigraphic analyses were carried out.

The collected data were organized into a geospatial database (QGIS Platform), in which each point represents an investigated site linked to a series of information as the precise location, the kind of volcanic sequence, and the stratimetric features (primary and secondary units, thickness, type of deposit, etc). The data were visualized using a Digital Elevation Model (DEM) of the Campanian Plain as reference topography and the UTM WGS 84 – Zone 33N reference projection.

3.3. Geomorphological analysis

https://doi.org/10.5194/egusphere-2023-1302
Preprint. Discussion started: 1 August 2023

This analysis is aimed at identifying the macro-basins that fed the lahars in the study area after the two sub-Plinian eruptions (Pollena and 1631). The analysis was carried out on the basis of the slopes distribution and the watersheds extracted from a Digital Elevation Model (DEM). The DEM was derived from a LiDAR flight of 2012 and stored with cell size of 10 m. In particular, six macro-basins characterized by slopes > 20° were identified in the Somma-Vesuvius area, whereas fifteen macro-basins with slopes > 25° were identified in the Apennines to the East of the volcano (Fig. 3). The different slopes thresholds are defined starting from previous studies (Pareschi et al., 2000, 2002; see also Bisson et al., 2013, 2014), and on the basis of a better analysis of the physical characteristics of the remobilized material, in turns related to the various types of deposits. In fact, along the slopes of Somma-Vesuvius, they are mainly ash-rich pyroclastic current deposits, while for the Apennines they are ash and lapilli fallout deposits emplaced along the variably-deep slopes. Each basin was considered as a single feeding unit for the lahars generation, and this is an input for the modeling of possible future lahars in the companion papers (de' Michieli Vitturi et al., submitted; Sandri et al., submitted).

https://doi.org/10.5194/egusphere-2023-1302
Preprint. Discussion started: 1 August 2023

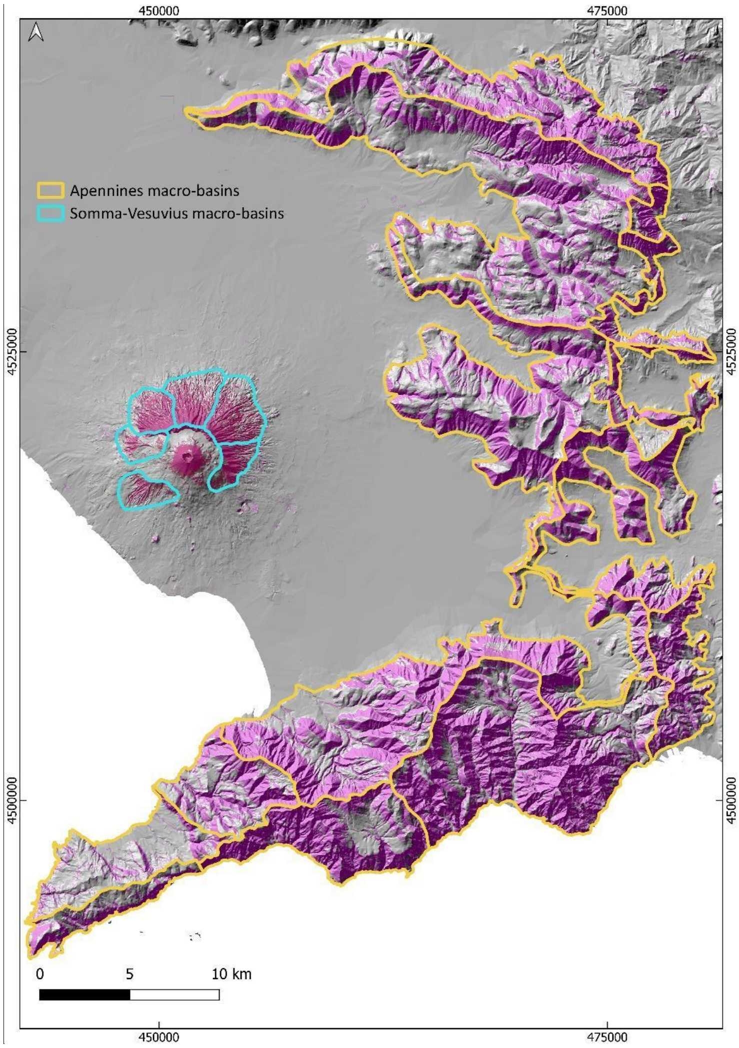

Fig. 3. The macro-basins defined on the basis of their geomorphological features to study the areas of possible accumulation and mobilization of deposits, which are used in modeling lahar generation of future events.

3.4. Laboratory and analytical work

3.4.1. Grain-size

In several sites among all the studied ones (Fig. 4), macroscopic analysis of the stratigraphic sequences was first carried out in the field to identify any homogeneities or similarities between the

https://doi.org/10.5194/egusphere-2023-1302
Preprint. Discussion started: 1 August 2023

juvenile fraction of the primary and secondary deposits, and recognize the various volcaniclastic units. This was followed by sampling the deposits and carrying out the laboratory analyses.

In particular, the sampling was mostly made on the syn-eruptive lahar deposits, but also on the post-eruptive and, in a few cases, on the primary pyroclastic deposits. All lab analyses were performed in the laboratories of sedimentology and optical microscopy at the Istituto Nazionale di Geofisica e Vulcanologia, Sezione di Napoli Osservatorio Vesuviano (INGV – OV). The material samples were pre-heated at a temperature of 60-70 °C to eliminate any fraction of humidity, then were quartered and sieved. To avoid any breaking of fragile clasts like pumices, the dry sieving of the grain-size classes between -4 (a coarse limit variable depending on the sample) and 0 phi was made manually, while for the classes between 0.5 and 5 phi a mechanical sieving apparatus was used.

The fine ash-rich deposit samples with high degree of cohesion were first combined with distilled water and thus boiled to remove all the ash aggregates, before being analyzed for granulometry following a wet procedure. In the post-processing of the data, the GRADISTAT excel package by Blott and Pye (2001) was used to determine the main statistical parameters. On selected samples, a microscopic componentry analysis was performed, consisting of recognizing and separating the various lithotypes that compose the volcaniclastic deposits, that is juvenile, lithic and crystal clasts. The clasts recognition was made manually for the coarser fractions, while for the finest fractions it was necessary the use of a reflected-light binocular microscope.

https://doi.org/10.5194/egusphere-2023-1302
Preprint. Discussion started: 1 August 2023

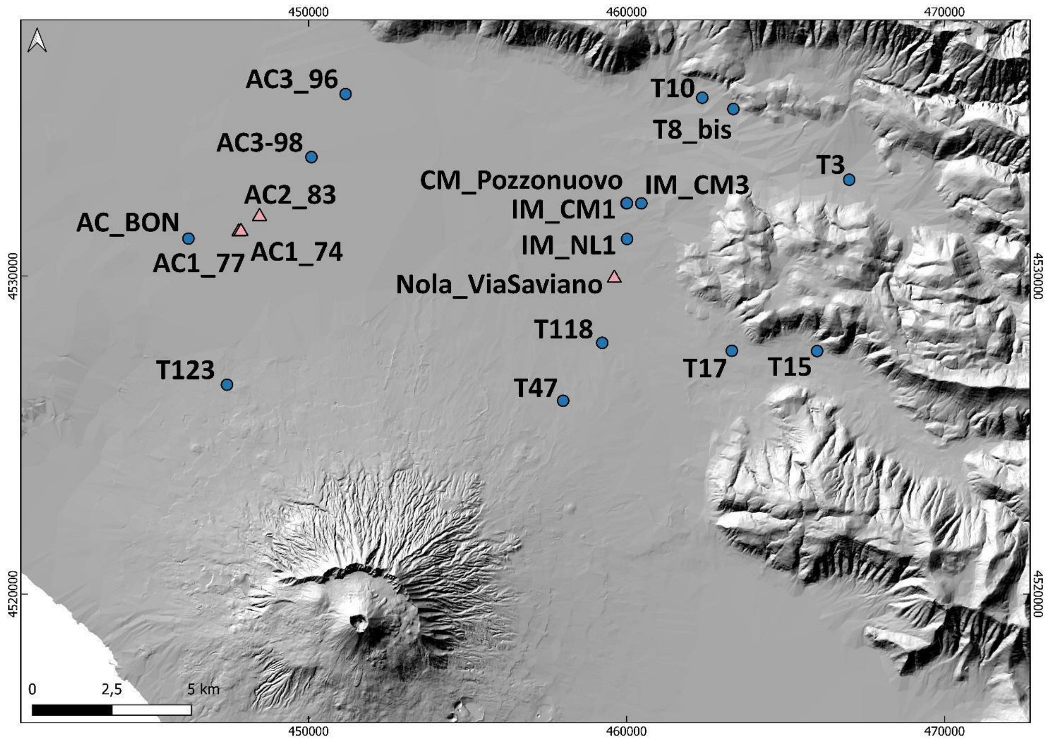

Fig. 4. Location of sites in which the sampling was carried out for sedimentological and paleomagnetic analyses. The pink triangles represent the sites for which a paleomagnetic study was carried out.

3.4.2. Input for impact parameters

A significant number of large clasts and boulders was also found embedded in the ash matrix of the lahar deposits at different locations. These clasts have dimensions from several centimeters to several tens of centimeters in diameter, and their nature is variable, that is limestone, ceramic, brick, tephra, lava, sandstone, iron (in order of abundance). Most of the clasts are fragments of artifacts from buildings, structures, and other archaeological finds of the Roman period, and their shape can be approximated in the field to ellipsoid. All these features suggest that they were entrained from substrate into the lahars to ultimately be deposited together with the ash. In the dynamics of volcaniclastic mass flows like lahars and pyroclastic currents, the occurrence of boulder entrainment

https://doi.org/10.5194/egusphere-2023-1302
Preprint. Discussion started: 1 August 2023

by flow dynamic pressure is recognized as a it is quite common feature (e.g., Zanchetta et al., 2004a; Pittari et al., 2007; Duller et al., 2008; Toyos et al., 2008; Cas et al., 2011; Carling, 2013; Doronzo, 2013; Jenkins et al., 2015; Roche, 2015; Martí et al., 2019; Guzman et al., 2020). The capability of a flow to entrain a clast is a function of flow properties (velocity, density) and clast properties (dimension, density, shape), and dynamic pressure well syntheses and quantifies such capability also in terms of flow hazard (Toyos et al., 2008; Zuccaro and De Gregorio, 2013; Jenkins et al., 2015). In Appendix 1, a theoretical scheme is presented to invert these field features for calculation of the impact parameters at local scale.

3.4.3. Rock magnetism

The lahar deposits related to the Pollena eruption were analyzed by rock magnetism at two localities, Acerra and Nola. We sampled both the deposit matrix and some potsherds embedded along three trenches (74, 77 and 83) and in the "Nola-Via Saviano" excavation (Fig. 4). The purpose of the magnetic measurements was threefold: i) evaluating the magnetic fabric of the deposits to infer the local to regional flow directions of the lahars and possibly their origin, whether Apennine or from Vesuvius; ii) estimating the deposition temperature (T_{dep}) of the deposits, to understand whether the lahar was triggered soon after the eruption or at later times; iii) testing the relative sequence (contemporaneity) of the lahars emplacement with respect to the Pollena eruption. All hand-samples were oriented *in-situ* with magnetic and solar compasses and reduced to standard sizes at the CIMaN-ALP laboratory (Peveragno, Italy), where all the magnetic measurements were made. In Appendix 2, the adopted paleomagnetic techniques are described.

4. Results

4.1. Field stratigraphy and sedimentological features

https://doi.org/10.5194/egusphere-2023-1302
Preprint. Discussion started: 1 August 2023

In this study, data of about 500 sites were collected, covering an area of >1000 km^2 from the plain around the volcanic edifice to the Apennine valleys to the north and east (Fig. 2).

4.1.1. Pyroclastic deposits: eruptions of Pollena and 1631

The integration of the collected data with the existing ones (Rosi and Santacroce, 1983; Rosi et al., 1993; Rolandi et al., 2004; Sulpizio et al., 2005; Perrotta et al., 2006; Bisson et al., 2007; Santacroce et al., 2008; Gurioli et al., 2010; De Simone et al., 2011) allowed the reconstruction of the distribution maps for both the fallout and pyroclastic current deposits. In particular, the spatial distribution highlights that for both the Pollena and 1631 primary deposits, thick fine ash deposits are widely distributed and cover the coarse fallout sequence or directly the ground, modifying the isopachs reconstructed by previous authors (Sulpizio et al., 2006 and references therein; Figs. 5 and 6). This enlargement of the area affected can have important implications on the hazard evaluation in terms of possible damages on a densely inhabited territory.

The area covered by the comprehensive isopach maps (including both the lapilli fallout and ash fallout) turns out to be wider than the one previously known, above all because we also took into account for the ash deposited by fallout during final stages of the eruptions, mostly dominated by phreatomagmatic explosions (Rosi and Santacroce, 1983; Sulpizio et al. 2005). The great distribution and availability of these ash deposits could explain the wide generation and distribution of the syn-eruptive lahars in the area. This has important implications in the evaluation of the source area and of the material available for lahars accompanying and following this eruption. In particular, there is an increase of the area covered by pyroclastic deposits and the calculated volume of the emitted products. For example, the area covered by the pyroclastic current deposits thus results in 200 km^2 for the Pollena eruption, and 120 km^2 for the 1631 eruption, while for the fallout deposits it is 433 km^2 and 427 km^2, respectively. Another implication is that the wide presence of fine and cohesive ash on top of the coarse fallout sequences and, in general on the ground, reduces the permeability of

https://doi.org/10.5194/egusphere-2023-1302
Preprint. Discussion started: 1 August 2023

the substrate, preventing the infiltration of the water and favoring the stream formation. They can also enhance the mobility of the flows by creating sliding surfaces.

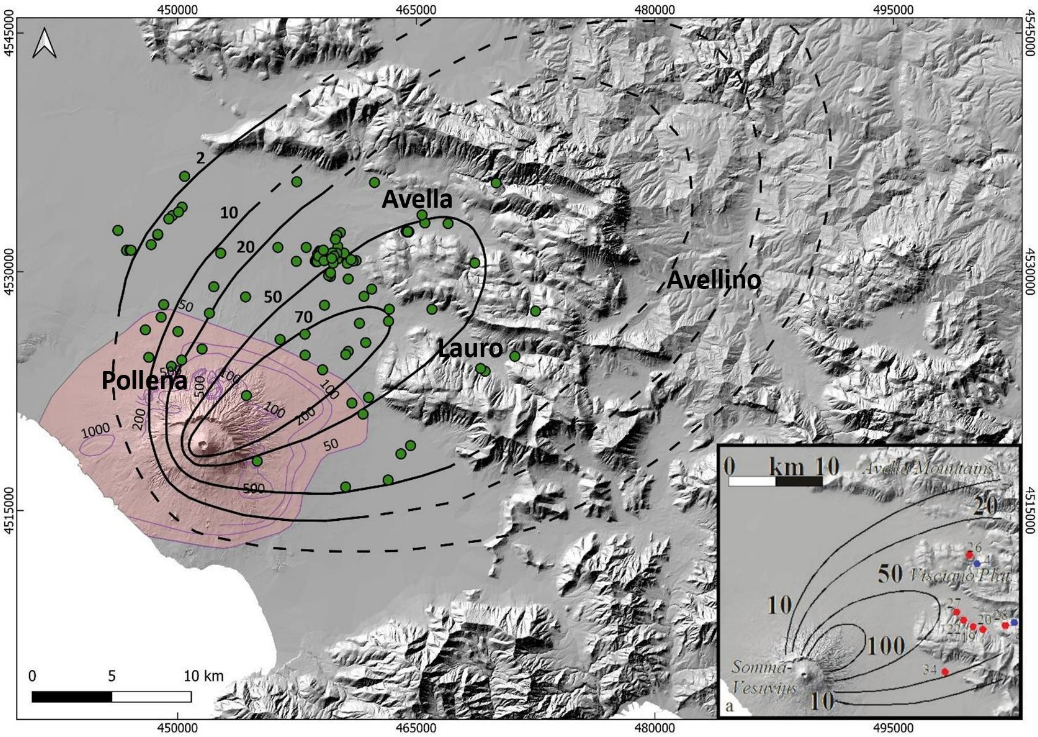

Fig. 5. Pollena eruption: the black lines represent the isopachs of the fallout deposits modified after Sulpizio et al., 2006 (in the insert) on the basis of the new collected data (green dots), while in pink is colored the area affected by PDC deposits, modified after Gurioli et al. (2010) (purple lines).

https://doi.org/10.5194/egusphere-2023-1302
Preprint. Discussion started: 1 August 2023

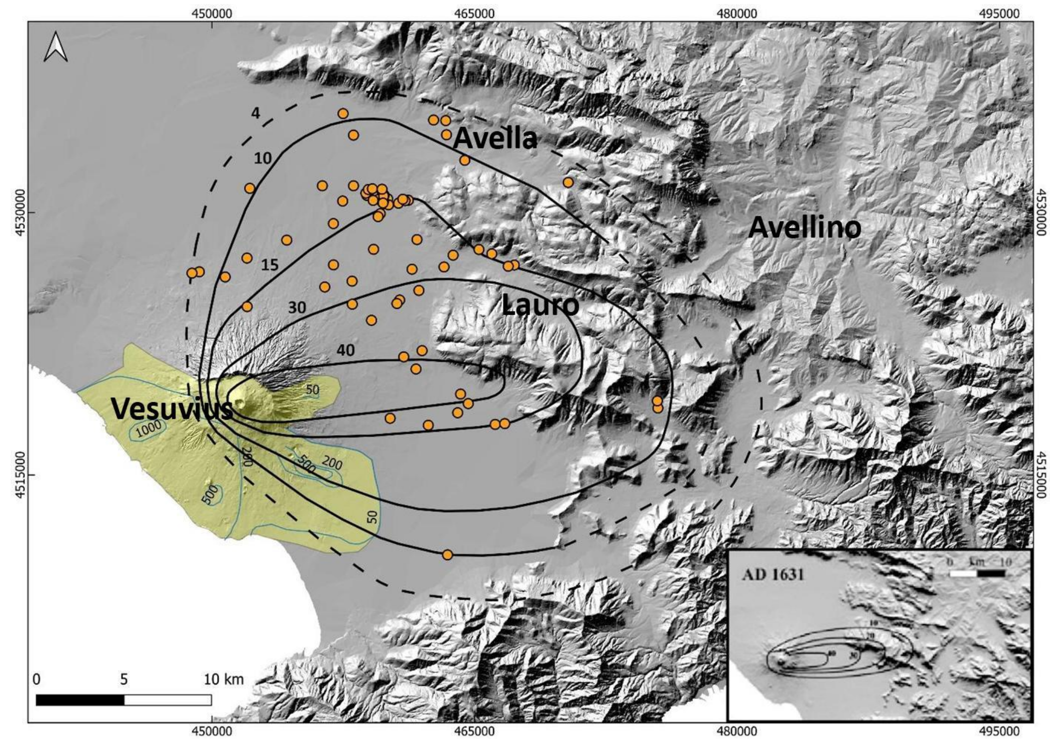

Fig. 6. 1631 eruption: the black lines represent the isopachs of the fallout deposits, modified after Santacroce et al., 2008 (in the inset) on the basis of the new collected data (orange dots), while in yellow is colored the area affected by PDC deposits. The light blue lines represent the inferred distribution on the basis of an integration between field data and fonts, modified after Gurioli et al. (2010).

The significant widening of the area affected by accumulation of the tephra fallout deposits, particularly towards the north for the 1631 eruption, follows the inclusion of the final ash deposits into the new isopachs. Interestingly, such widening agrees with the wide occurrence of lahars in the plain north of Vesuvius, as documented in the chronicles and sources (Rolandi et al., 1993; Rosi et al., 1993, and references therein), and as follows.

4.1.2. Lahar deposits

https://doi.org/10.5194/egusphere-2023-1302
Preprint. Discussion started: 1 August 2023

The lithological and sedimentological analyses allowed the definition of the primary pyroclastic deposits involved in the remobilization. In many cases, the archaeological findings permitted to define the local paleoenvironment and the land use, and also to constrain the age and timing of deposition. The lithofacies mostly recognized are P to indicate paleosoil and humified surface, mL and mA (massive lapilli and massive ash, respectively) to indicate the primary deposits, while the lahar deposits usually belong to the facies Gms and mM, which indicate massive, matrix-supported gravel deposits and massive lahar deposits, respectively. Other recognized lithofacies are Sh, Ss and fM. Sh indicates hyper-concentrated flow deposits, and consists of an alternation of coarse and fine beds. Ss includes scour and fill structures, and consists of an erosive, concave-upwards basal surface and a planar/convex top. fM is fine mud, and indicates the decantation deposit formed when the flow loses its energy.

Usually, the syn-eruptive lahar deposits directly overlie the primary deposits, sometimes eroding them. They have a matrix-supported texture and are composed of fine to very fine cohesive ash, and contain scattered and more or less abundant pumices and lithic fragments. They are generally composed of multiple depositional units, each one resulting from single “en masse” transport. The different flow units are distinguishable (still in continuity) from each other based on vertical granulometric changes, pumice alignments, internal lamination and/or unconformities. Compared, for example, with channeled pyroclastic currents, dense water flows and floods, such units could have been repeatedly emplaced under accumulation rates of several tens to a few hundreds kg/m^2s (Lowe, 1988; Russell and Knudsen, 1999; Whipple et al., 2000; Girolami et al., 2010; Roche, 2015; Marti et al., 2019; Guzman et al., 2020). In various areas, the “en masse” transport is suggested by the presence of water escape structures through the whole deposit and sequence of units. These are vertical structures consisting of small vertical “pipes” filled by fine mud, transported by the escaping water, formed soon after the emplacement of the lahar. The lithological characteristics are variable even within the same site, but the deposits are generally massive, contain vesicles from circular to flattened and coated by fine ash. For the syn-eruptive lahar deposits, the fragments are those of the primary

https://doi.org/10.5194/egusphere-2023-1302
Preprint. Discussion started: 1 August 2023

deposits, while in the upper parts of the sequences it is not uncommon to find units that contain pumices fragments related to previous eruptions, in particular the 9.0 ka B.P "Mercato" and the 3.9 ka B.P. "Avellino" Plinian eruptions. In this case, these deposits are considered post-eruptive. Also, the presence in the sequences of slightly humified surfaces or evidence of human artifacts, such as for example excavations, plowing, etc, are considered as constraints for a long non-deposition, and lahars generation is considered as post-eruptive. In other words, the componentry of the secondary vs. primary pyroclastic deposits for the two sub-Plinian eruptions, as well as the vertical continuity between the fallout and lahar deposits, are strong indicators of the syn-eruptive occurrence of the lahar events. Instead, the absence of such features is more indicative of a post-eruptive origin, with lahars events also more spaced in time from the corresponding eruption.

In Appendix 3, a description is reported for some of the most representative sequences, which were sampled in different areas throughout the plain (Figs. 2 and 4).

4.1.3. Distribution maps of the lahar deposits

Here we present the distribution maps for the lahar deposits of the eruption of Pollena and 1631 (Figs. 7-10). In particular, the syn-eruptive Pollena lahar deposits are distributed in the NW quadrants of the volcano and in the Avella, Lauro and Sarno valleys (see Fig. 1), with a thickness exceeding 1 m in the Vesuvius apron and in the plain between Nola and Cimitile (see Figs. 1 and 7). A volume estimation of the remobilized deposits is 73×10^6 m^3 for the northern Vesuvius area and 42×10^6 m^3 for the Lauro Valley.

https://doi.org/10.5194/egusphere-2023-1302
Preprint. Discussion started: 1 August 2023

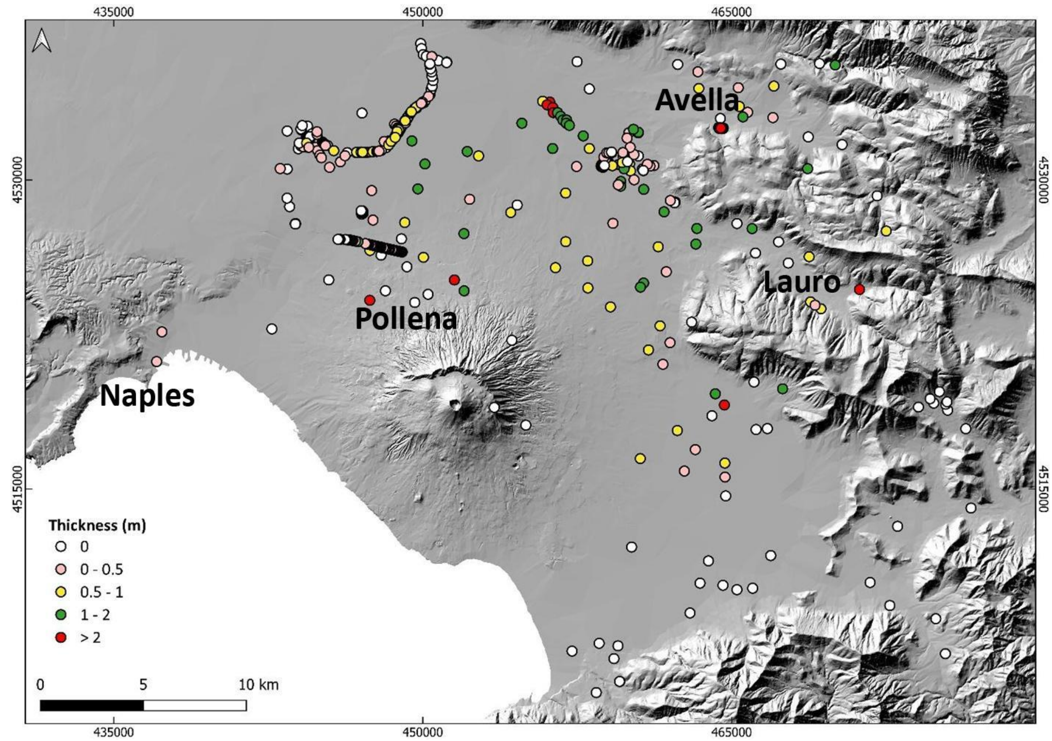

Fig. 7. Distribution of the syn-eruptive lahar deposits related to the Pollena eruption.

The post-eruptive deposits of the Pollena eruption are more concentrated in the Avella and Lauro valleys, and in the plain north of the volcano close to the apron area (low-angle edifice outer slopes) (Figs. 1 and 8). Their deposits contain both fragments from the Pollena eruption and from preceding eruptions, suggesting that pyroclastic deposits of the older sequences were progressively eroded and involved in remobilization processes over time. As an example, in Figs. A3a-d it is possible to recognize whitish pumice fragments from the Pomici di Avellino and Mercato eruptions on top the Pollena lahar deposits.

https://doi.org/10.5194/egusphere-2023-1302
Preprint. Discussion started: 1 August 2023

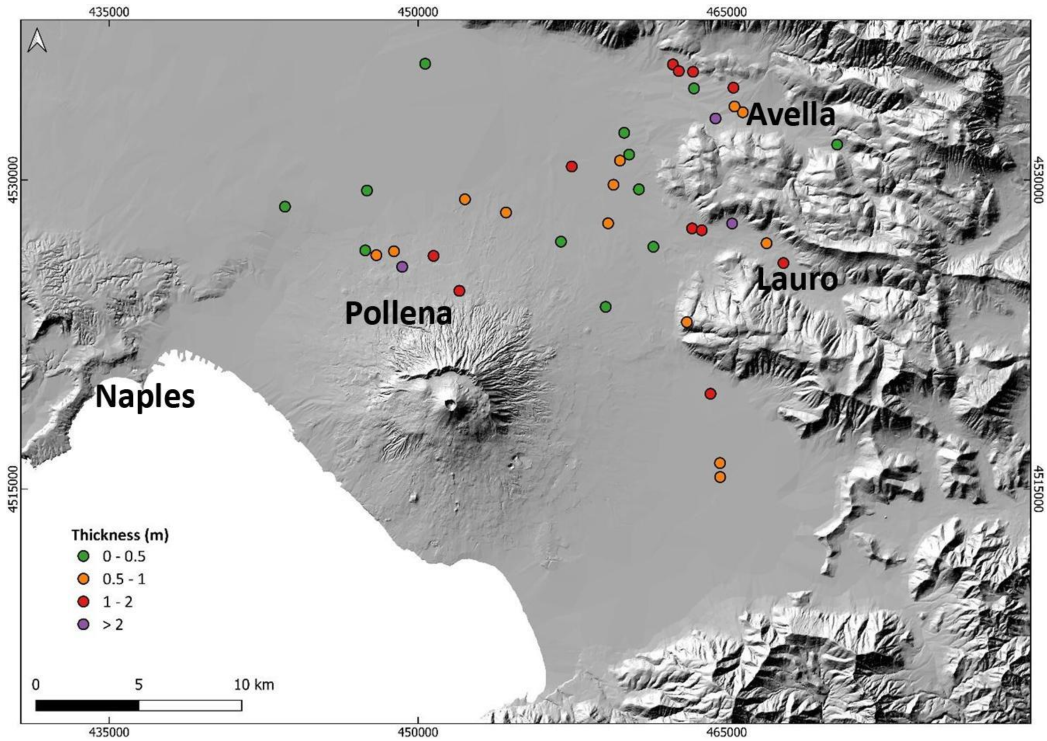

Fig. 8. Distribution of the post-eruptive lahar deposits related to the Pollena eruption.

Above the Pollena primary and secondary deposits (meaning after the emplacement of the Pollena lahars), the studied sequences in almost all the sites show the presence of a well-developed soil bed with many traces of cultivation, as well as of the presence of inhabited areas and buildings (Figs. A3a-d). These traces and the presence of a well-developed soil bed are evidence of a progressive geomorphological stabilization of the territory. The occurrence of the 1631 sub-Plinian event determined a new phase of marked geomorphological instability for a large territory surrounding the volcano. In Fig. 9, it is shown the distribution of the syn-eruptive lahar deposits in all the studied areas with variable thickness, generally <50 cm. They affected mostly the areas of Acerra-Nola, Sarno, the Vesuvius apron and the Apennine valleys (Figs. 1 and 9). Rosi et al. (1993) and Sulpizio et al. (2006) reported that floods and lahars heavily impacted (also with injuries and victims) the N and NE quadrants of Somma-Vesuvius soon after the eruption with a timescale of days (Rosi et al.,

https://doi.org/10.5194/egusphere-2023-1302
Preprint. Discussion started: 1 August 2023

1993; see also the historical chronicles of Braccini, 1632), corroborating the syn-eruptive behavior of such lahars. Furthermore some lahars are also intercalated within the primary pyroclastic deposits, while generally they stand in continuity on top of the primary deposits (Rosi et al., 1993); both cases unequivocally constrain the syn-eruptive behavior of the 1631 lahars.

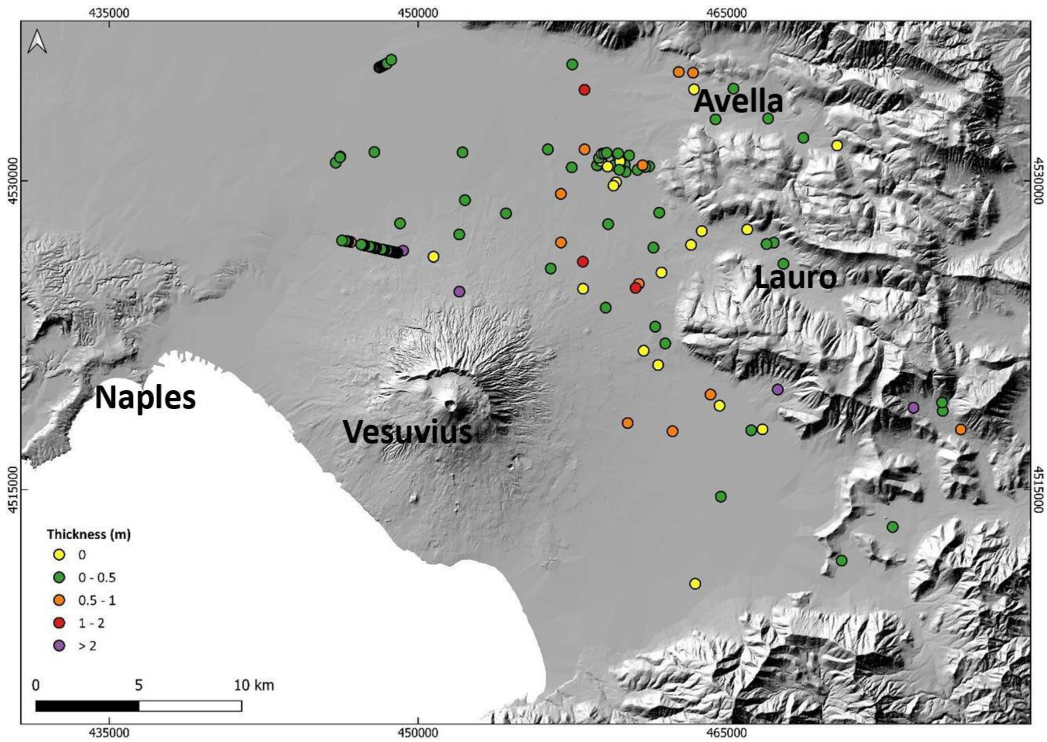

Fig. 9. Distribution of the syn-eruptive lahar deposits related to the 1631 eruption.

Minor post-eruptive lahar deposits of the 1631 eruption are reported in Fig. 10, with a preferential distribution to the E quadrants of the volcano from N to S, both in the plain and the valleys. These deposits are still significant, with a thickness of around half a meter to a meter or more in a few points.

https://doi.org/10.5194/egusphere-2023-1302
Preprint. Discussion started: 1 August 2023

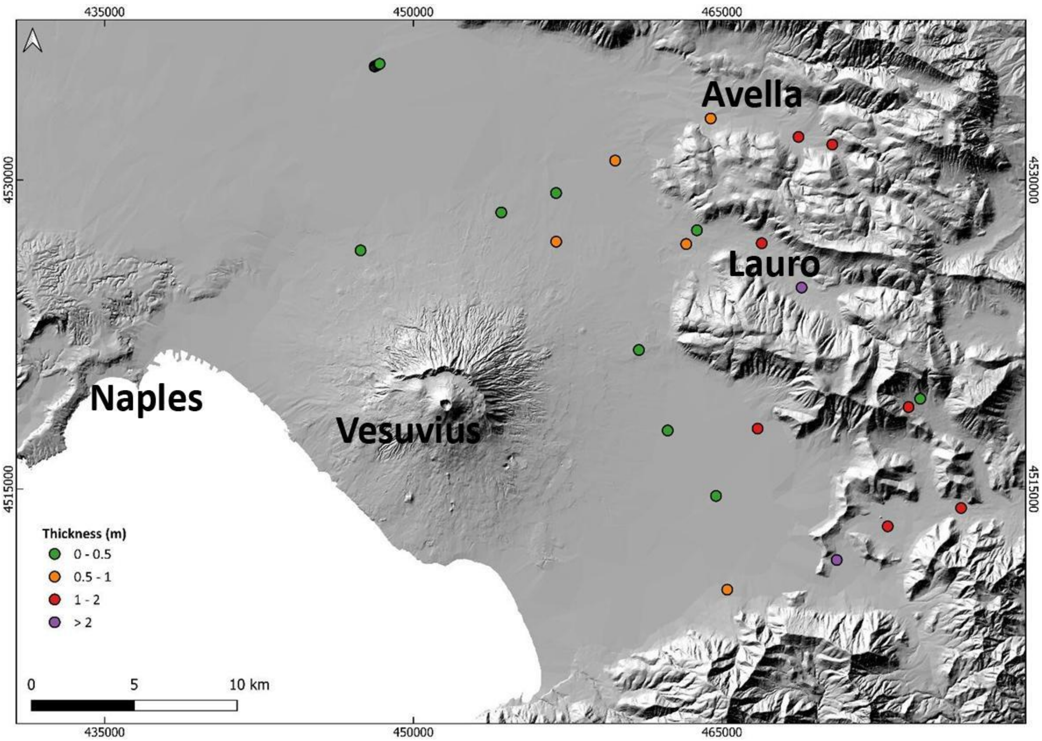

Fig. 10. Distribution of the post-eruptive lahar deposits related to the 1631 eruption.

4.1.4. Sedimentological characteristics of the Pollena lahar deposits

The field analysis carried out on about 500 studied sites, and the laboratory analysis carried out on 30 selected samples contribute both to the distinction between syn- and post- eruptive lahars in the area. The results of the grain-size analyses in the form of histograms and statistical parameters are presented in Fig. 11 and Tab. 1.

The juvenile pumice clasts are an ubiquitous component of deposits, but they decrease with distance toward the finer grain-size classes, while the crystal content increases in the same progression. The lithic clasts are abundant in the coarser classes, they decrease with distance in the middle grain-size classes, and increase again in the finer classes.

https://doi.org/10.5194/egusphere-2023-1302
Preprint. Discussion started: 1 August 2023

Vallo di Lauro

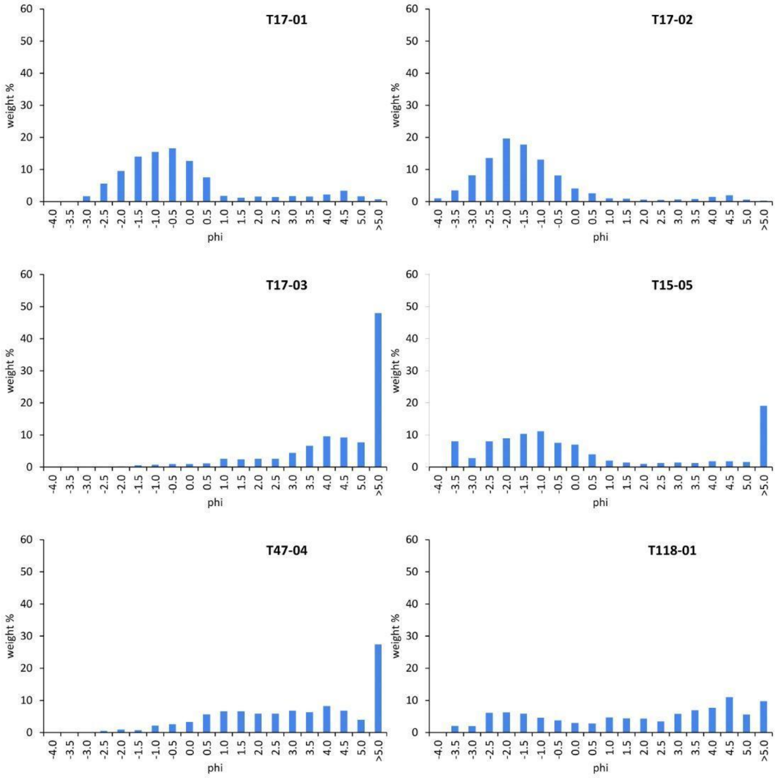

Somma-Vesuvius

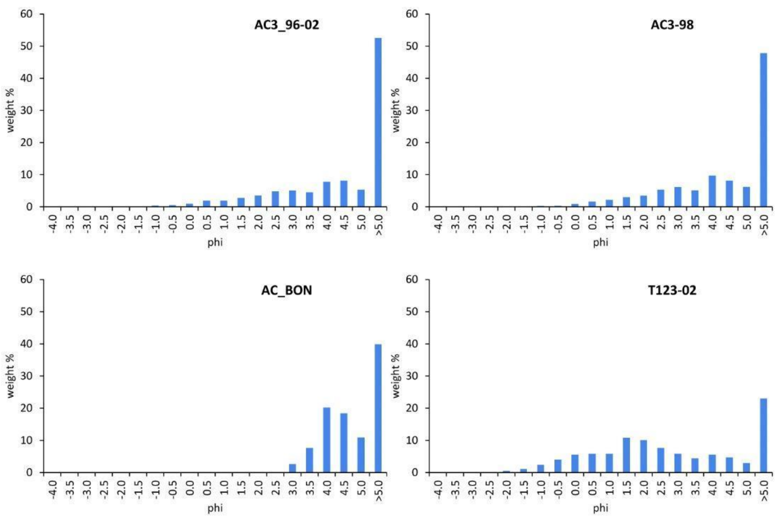

https://doi.org/10.5194/egusphere-2023-1302
Preprint. Discussion started: 1 August 2023

Valle di Avella

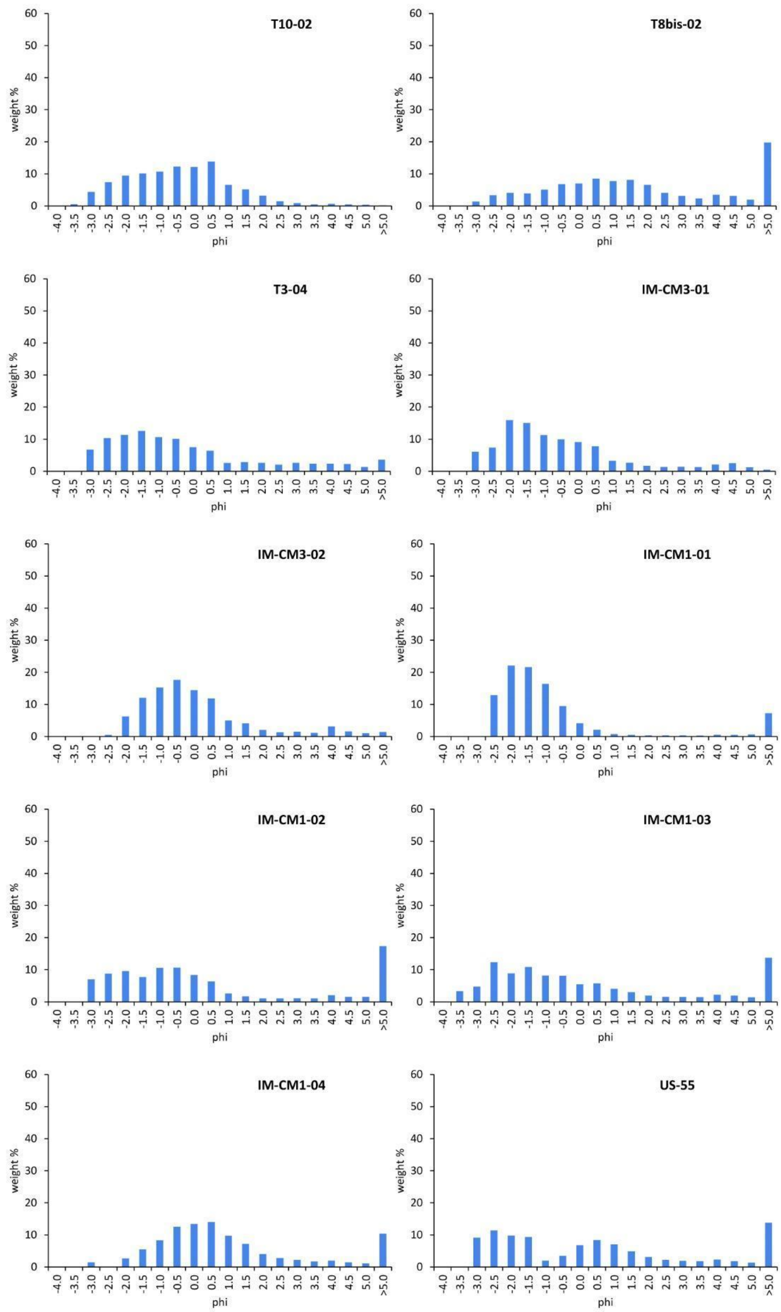

https://doi.org/10.5194/egusphere-2023-1302
Preprint. Discussion started: 1 August 2023

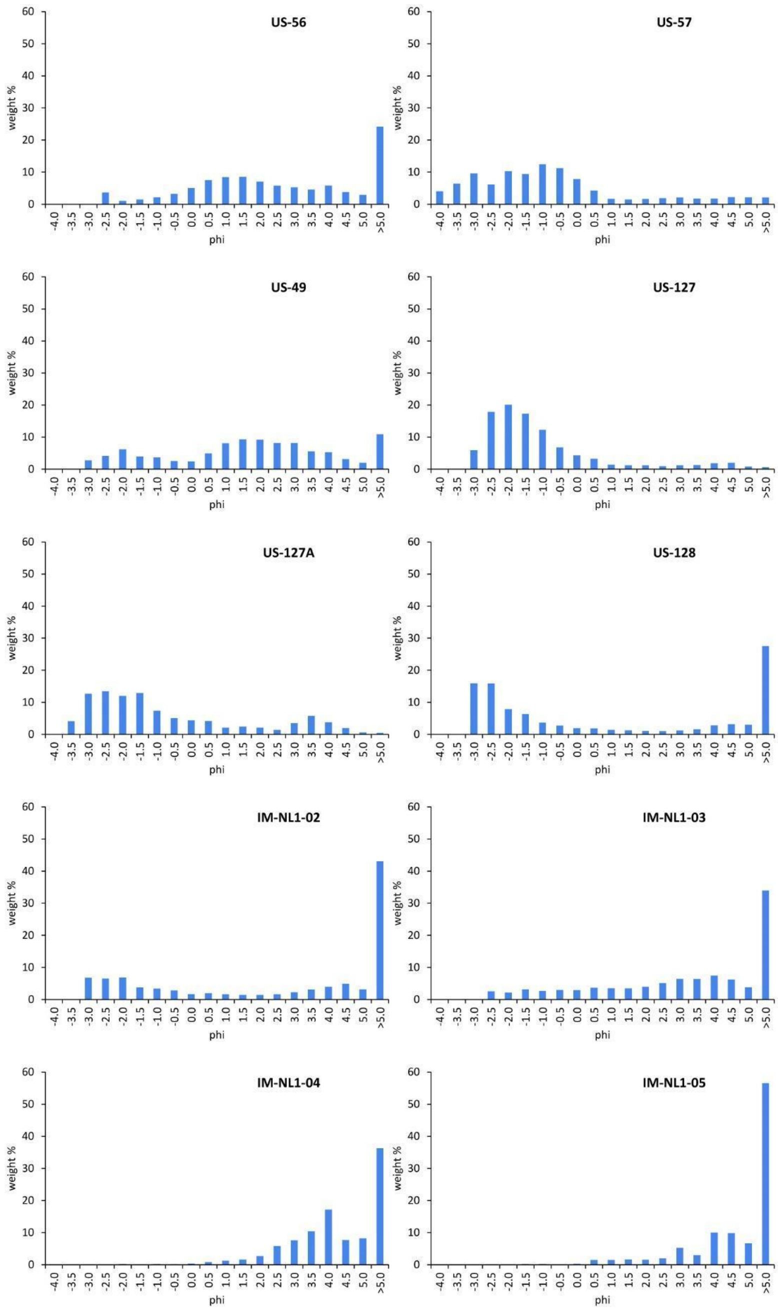

Fig. 11. Histograms of the grain-size analysis on selected samples for the locations reported in Fig. 4.

SAMPLE	MODE 1	MODE 2	MODE 3	SKEWNESS	SORTING	FACIES
Lauro Valley						
T17-01	-0.743			1.179	1.464	Gms
T17-02	-2.243			1.532	1.404	Gms
T17-03	0.747	3.731		-1.054	1.481	Sh
T15-05	-3.743	-1.243	3.731	0.890	1.752	Gms
T47-04	1.247	3.731		-0.447	1.579	Mm
T118-01	-2.243	0.747	3.731	-0.049	2.352	Gms
Avella-Baiano Valley						
T10-02	0.247			0.274	1.457	Sh
T8bis-02	-2.243	0.247	1.247	-0.009	1.742	Sh
T3-04	-1.743	1.247	3.237	0.881	1.789	Gms
IM-CM3-01	-2.243			1.015	1.587	Gms
IM-CM3-02	-0.743	3.731		1.134	1.379	Gms
IM-CM1-01	-2.243			1.954	1.010	Gms
IM-CM1-02	-2.243	-1.243	3.731	0.932	1.633	Gms
IM-CM1-03	-2.743	-1.743	0.247	0.810	1.809	Gms
IM-CM1-04	0.247			0.406	1.394	Fm
US-55	-2.743	0.247	3.731	0.495	1.941	Gms
US-56	-2.743	1.247	3.731	-0.402	1.700	Sh
US-57	-3.243	-2.243	-1.243	0.756	1.860	Gms
US-49	-2.243	1.247		-0.460	2.012	Gms
US-127	-2.243			1.686	1.507	Gms
US-127A	-2.743	-1.743	3.237	0.914	2.167	Gms
US-128	-3.243	3.731		1.434	1.990	Gms
IM-NL1-02	-3.243	-2.243	3.731	0.609	2.378	Gms
IM-NL1-03	-1.743	0.247	3.731	-0.458	1.996	Gms
IM-NL1-04	3.731			-1.698	0.995	Mm
IM-NL1-05	1.247	2.737	3.731	-1.137	1.224	Mm
Somma-Vesuvius						
AC3_96-02	0.247	2.237	3.731	-0.734	1.245	Mm
AC3-98	2.737	3.731		-0.838	1.197	Mm
AC_BON	3.731			-3.026	0.425	Mm
T123-02	0.247	1.247	3.731	-0.228	1.420	Mm

Tab. 1. Statistical parameters extracted from the grain-size analyses. Mode 1, 2 and 3 indicate the coarsest, medium and fine modes, respectively.

https://doi.org/10.5194/egusphere-2023-1302
Preprint. Discussion started: 1 August 2023

Field observations and statistical granulometric parameters (modes, skewness, sorting), highlight significant differences between the sectors of Lauro Valley, Avella-Baiano Valley, and Somma-Vesuvius. A common feature between the three sectors is that the lahar deposit samples are mostly massive, poorly-sorted and polimodal; only a few samples are moderately-sorted and unimodal. On the other hand, the grain-size modes extracted show some interesting differences. The coarse modes for Lauro Valley and Avella-Baiano Valley span from fine/medium lapilli to coarse ash, while for Somma-Vesuvius span from coarse to fine ash. The medium modes for Lauro Valley and Avella-Baiano Valley span from coarse to medium ash, while for Somma-Vesuvius span from medium to fine ash. The fine modes for Lauro Valley and Avella-Baiano Valley, and for Somma-Vesuvius span from medium to fine ash. Also, the skewness values for Lauro Valley and Avella-Baiano Valley show a fine-to-coarse mode while for Somma-Vesuvius show a coarse code. All these differences basically depend on the origin of the primary pyroclastic deposits, fallout vs. pyroclastic currents, which were remobilized from different sectors, Apennines and Somma-Vesuvius. The analysis of the above described granulometry is used to inform the model of lahar transport (de' Michieli Vitturi et al., submitted) aimed at assessing the related hazard (Sandri et al., submitted).

4.2. Magnetic results

Both Acerra and Nola localities show a well-defined magnetic fabric. Principal susceptibility axes are clustered, and the magnetic anisotropy Pj is mostly lower than 1.060 but can reach high values (P = 1.200). At Acerra, the magnetic foliation is always dominant, and the fabric is oblate. The Pj is linearly correlated to the mean susceptibility (k_m). The magnetic fabric has a horizontal magnetic foliation and a clustered magnetic lineation, whose mean direction is NE-SW. Considering the chaotic nature of the lahar deposits, the high Pj and the clustered susceptibility axes can highlight a channelized flow (Fig. 12). At Nola, instead, the fabric is both prolate/oblate, and Pj is lower than 1.040. The susceptibility axes are more dispersed than Acerra, but mean magnetic lineation clearly

https://doi.org/10.5194/egusphere-2023-1302
Preprint. Discussion started: 1 August 2023

shows a NW-SE direction. If one considers the oblate specimens only, the magnetic foliation is sub-horizontal, on the contrary, the magnetic foliation of the prolate specimens is steeply dipping (65°) toward SE. At Nola, the flow direction inferred by AMS is consistent and parallel to the invasion basin.

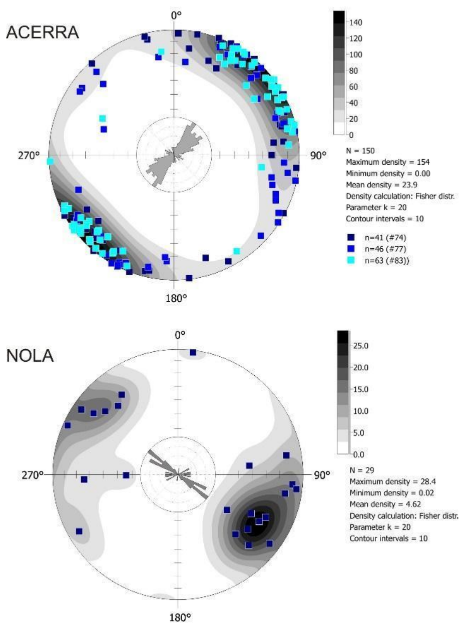

Fig. 12. Equal area projection and Rose diagram of the K_1 directions at Acerra and Nola.

The deposition temperature is low at both deposits. At Acerra the T_{dep} interval is 120-140 °C, while for Nola T_{dep} is lower than 120 °C (Fig. 13). In the Nola case, a low temperature magnetization component lower than 120 °C cannot be directly considered as a TRM. In fact, the low T_b Earth's field component of magnetization can also be produced by a viscous remanent magnetization (VRM), acquired during exposure to weak fields (Bardot and McClelland, 2000). The acquisition of the VRM depends on the duration of the exposure. For age around that of the Pollena eruption, the minimum T_{dep} which can be distinguished is ca. 120 °C. For this reason, we considered the Nola lahar to be emplaced at low temperature.

https://doi.org/10.5194/egusphere-2023-1302
Preprint. Discussion started: 1 August 2023

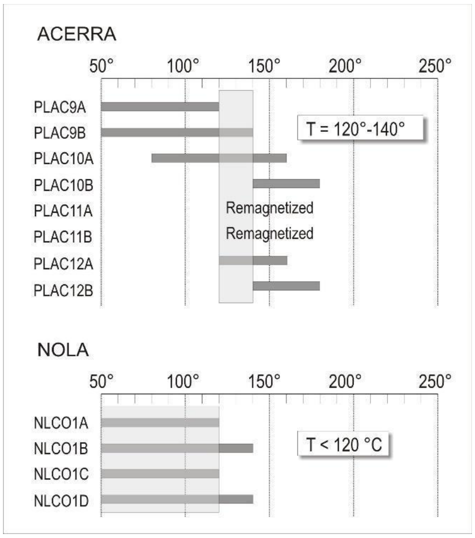

Fig. 13. Deposition temperature at Acerra and Nola. The site T_{dep} is estimated from the overlapping reheating temperature ranges for all lithic clasts sampled.

The mean paleomagnetic direction for each locality, calculated using Fisher's statistics, is well-defined and is statistically distinguishable at the 95% confidence limit (Fig. 14). Therefore, the lahar deposits of these two localities are not synchronous.

Overall, all magnetic measurements just discussed show distinctly different characters between Acerra and Nola, clearly indicating two distinct events of emplacement.

https://doi.org/10.5194/egusphere-2023-1302
Preprint. Discussion started: 1 August 2023

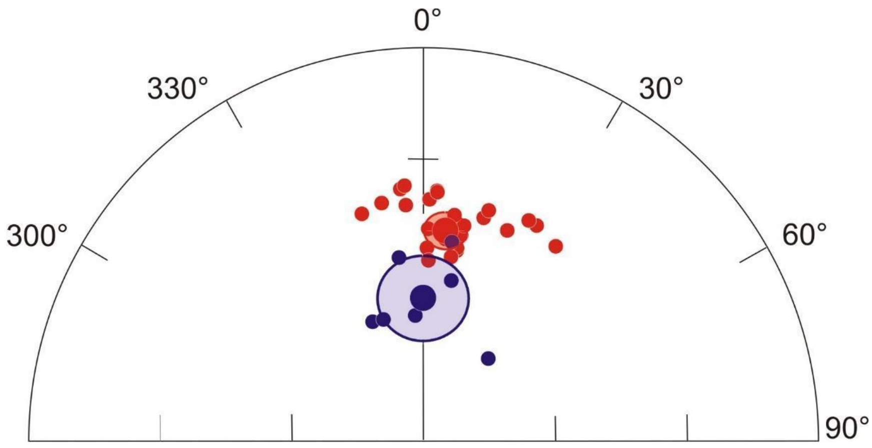

Fig. 14. Equal-area projection of the characteristic remanent magnetization directions, and their mean value with associated confidence limit, from Acerra (red dots, mean value: n=26 D=7.5°, I=43.4°, alpha95=3.5°), and Nola (blue dots, mean value: n=7, D=0.8°, I=60.2°, alpha95=9.0°).

4.3. Lahar dynamics

By inverting the field evidence and data, it is possible to reconstruct the macroscopic flow dynamics that occurred in the lahar invasion, which are particularly interesting to understand the impact that those lahars had on the Vesuvius territory. As already described, the lahar deposits show thicknesses that are variable from several centimeters to a few meters, and this can depend on multiple local factors: i) topography; ii) distance from source; iii) erosion; iv) source area and type of remobilized sediment (variably sized fallout vs. flow deposits). In particular, thicker deposits are found near the mouth of the valleys and in the flat alluvial plain, as shown in the deposit distribution maps. On the other hand, the deposits show on the whole a tabular-like shape, and the average thickness is of the order of 0.5-1 m, which is the first evidence of the lahars impact. In terms of runout distance, the lahars traveled for 10 to 15 km from sources (Somma-Vesuvius and Apennine detachment areas), measured directly on the deposit distribution maps. These important quantitative constraints are used to validate and inform lahar numerical models (de' Michieli Vitturi et al., submitted) and simulations (Sandri et al., submitted) for hazard assessment. We cannot rule out that lahar pulses from different

https://doi.org/10.5194/egusphere-2023-1302
Preprint. Discussion started: 1 August 2023

source areas (Somma-Vesuvius vs. Apennines) might have overlapped in the open plain. At several locations, we found erosive unconformities between (Fig. 15a) the lower and upper flow units (Fig. 15b), as well as between primary pyroclastic deposits and lahar units. Erosion is an important factor for the entrainment of preexisting material including large-size clasts. Size and density of the largest clasts embedded in the deposits can give an idea of the carrying capacity of the lahars.

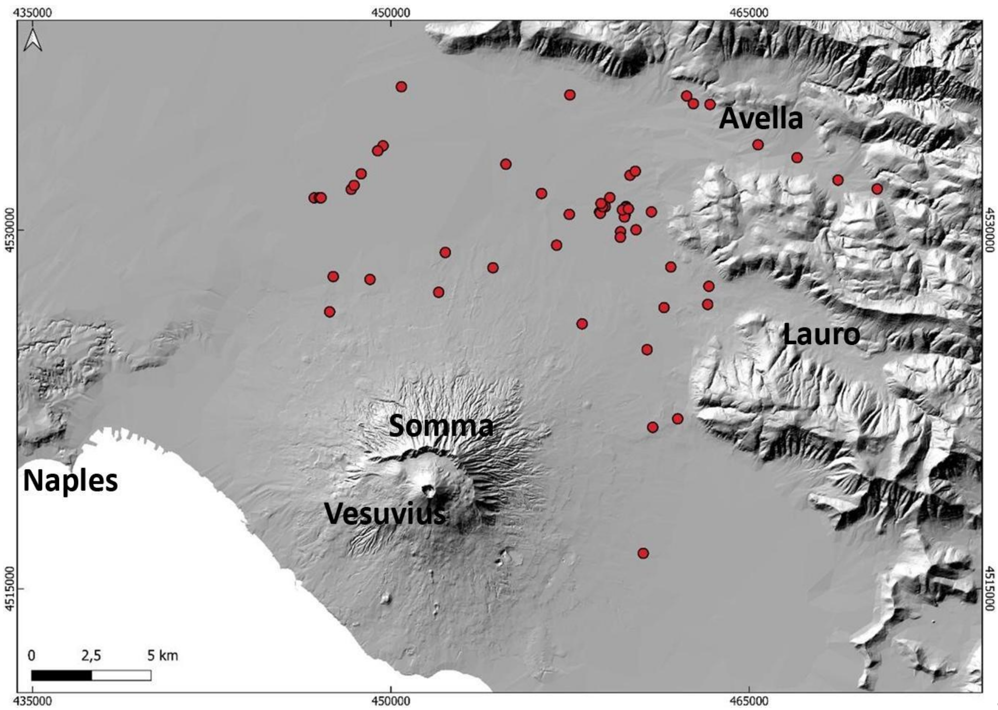

a)

https://doi.org/10.5194/egusphere-2023-1302
Preprint. Discussion started: 1 August 2023

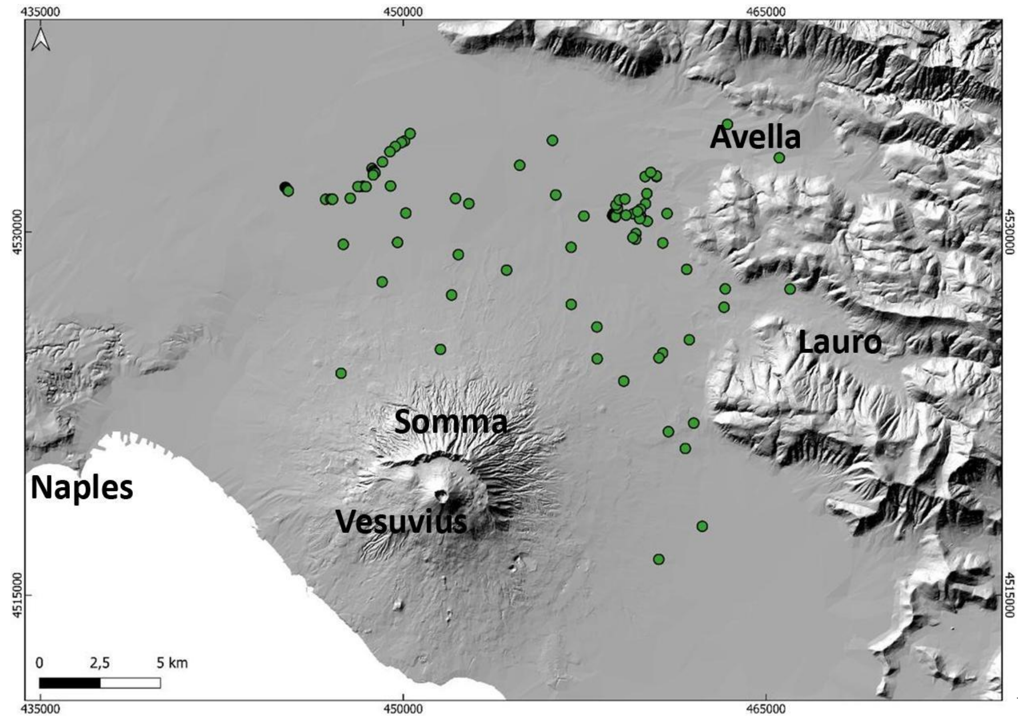

b)

Fig. 15. a) Sites with evident erosion traces at the base of the lahar units; b) Sites in which multiple flow units are vertically identified.

Evidence of oversize clasts are observed in all the studied areas, with a distribution that is similar to the one of the deposits themselves (but with less proportions), and particularly at the mouth of the valleys, and in the alluvial plain (Fig. 15a). The presence of the erosional features, and the fact that the deposits are ubiquitously massive, suggest that high transport and deposition were not exclusive processes, i.e. they both occurred even at local scale.

We calculated local velocities of the syn- and post-eruptive lahars based on the biggest clasts that are found in the deposits, with dimensions from several centimeters to a meter, and for flow density ≥ water density (Appendix 1).

https://doi.org/10.5194/egusphere-2023-1302
Preprint. Discussion started: 1 August 2023

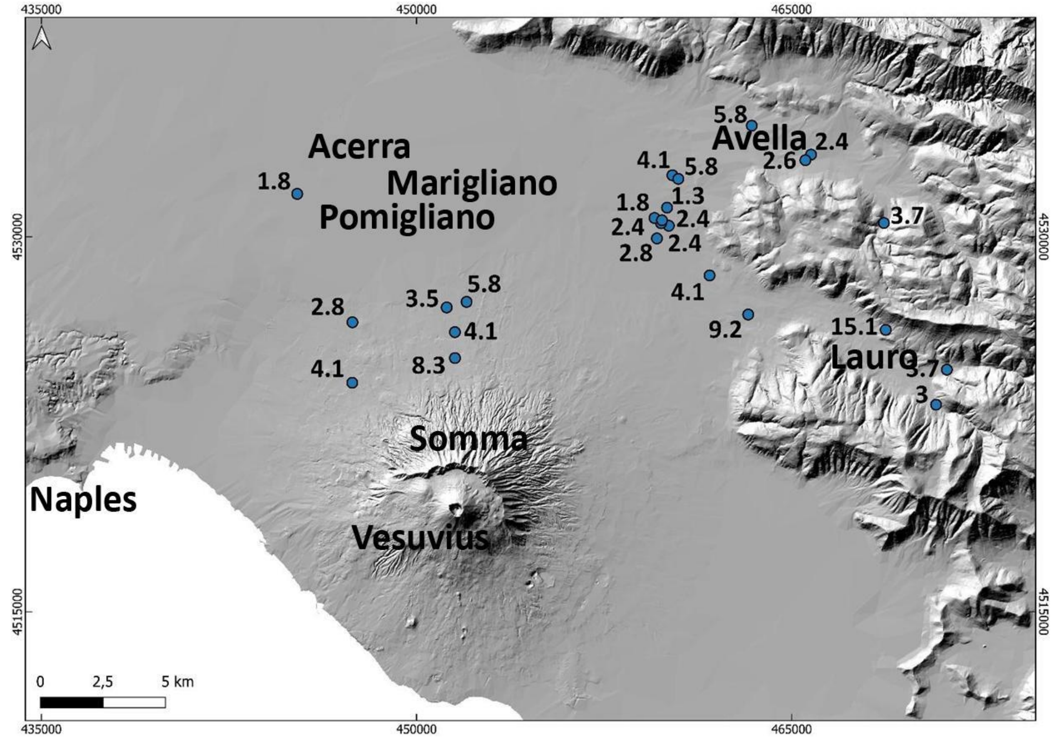

Fig. 16. Average lahar velocities (in m/s) estimated with a point-by-point reverse engineering approach.

Then, we used the flow velocities (Fig. 16) to calculate local dynamic pressures of the lahars (Fig. 17) as a function of the clast properties. The obtained estimations are used by Sandri et al. (submitted) to validate the Probabilistic Hazard Assessment of lahars from Vesuvius eruptions.

https://doi.org/10.5194/egusphere-2023-1302
Preprint. Discussion started: 1 August 2023

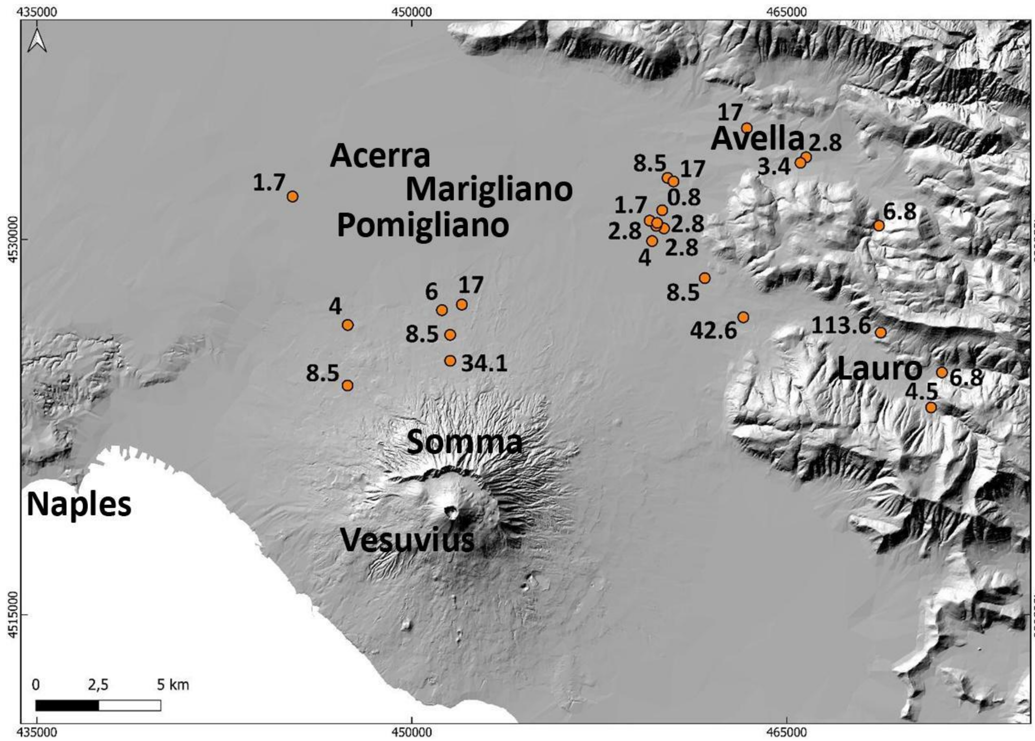

Fig. 17. Average lahar dynamic pressures (in kPa) estimated with a point-by-point reverse engineering approach.

The data presented in Figs. 16 and 17 represent respectively minimum local values of the flow velocity and dynamic pressure, useful to assess some minimum impact of the lahars in the alluvial plain. In particular, we did a parametric test to quantify the sensitivity for different physical states of the multiphase flow, considering two end members, from a non-fluidized case to an initially fluidized and non-expanded case (see Appendix 1). From the performed analysis (see Appendix 1) we found that the most typical values are referred to the initially fluidized and slightly expanded case, with most of the points falling in the range of velocity of 2-4 m/s, and dynamic pressure of 4-8 kPa.

Lastly, in eight points we found the lahar deposits against meter-sized obstacles, from which we estimated, by comparison, local flow heights of the order of 1-1.5 m, and particle volumetric concentrations of ~30% or more, i.e. the deposit thickness is ~1/3 of the lahar thickness. On the other hand, it is reasonable to argue that these are local values, and that flow height, particle concentration,

https://doi.org/10.5194/egusphere-2023-1302
Preprint. Discussion started: 1 August 2023

and deposit thickness significantly varied over space due to the multiphase nature of the lahars (see de' Michieli Vitturi et al., submitted; Sandri et al., submitted).

5. Discussion

The historical sources used as benchmark for the problem of the lahars around Somma-Vesuvius and in the Apennine valleys remark the frequent and broad impact that explosive eruptions of Vesuvius had in historical times. Some of the eruptions occurred in the last four centuries (e.g., 1631, 1822, 1906 and 1944) reached contemporaneously and repeatedly over time a number of municipalities due to the explosive character of the events, particularly in the sub-Plinian eruption of 1631. Heavy rain events caused remobilization of the primary deposits, triggering multiple lahars during or immediately after the eruption up to a few years (syn-eruptive lahars).

On the other hand, the 472 Pollena eruption had an even wider impact, both in terms of primary pyroclastic deposition and secondary (lahar) impact. For this event the sources are scarce or absent.

The analysis of – and realization of a database with – more than 500 stratigraphic sections were done, which also includes the sedimentological features both of primary (fall, flows) and secondary (lahars, alluvial events) deposits relative to the two sub-Plinian eruption case studies from Vesuvius, Pollena and 1631. The detailed reconstruction and mapping of these deposits allow an updating of the pyroclasts distribution on the territory, as both the eruptions had an impact larger than previously known. In particular, the stratigraphic and sedimentological reconstruction of the deposits was done not only in open spaces but also close to urban areas, and this is important in terms of local impact of the lahars vs. broad impact in the environment. Specifically, such impact investigation was done in urban areas including archaeological findings (e.g., villages, structures, walls, etc).

These findings include not only new data from the Somma-Vesuvius plain but also more distal deposits from Lauro Valley and Avella-Baiano Valley (Apennines), which were subjected to heavy remobilization also of the finer primary deposits as for the presence of fine ash deposits present in

https://doi.org/10.5194/egusphere-2023-1302
Preprint. Discussion started: 1 August 2023

both proximal and distal areas. Indeed, the accumulation areas that were reconstructed reveal an enlargement and extra 20% coverage that was not previously known and, considering the physical characteristics of the ash, it should be considered in any hazard and impact evaluation. The full database thus allows a more precise reconstruction of the new isopachs, both for the Pollena and 1631 eruptions, which is possible given the high number of data points.

With particular reference to the lahar deposits, the syn-eruptive ones that were emplaced by relatively short-term (during or immediately after the eruption) events stand directly on the primary pyroclastic deposits both for Pollena and 1631 eruptions case-studies. Also, there are not any erosion surfaces due to prolonged exposure of the primary, testifying that the secondary emplacement was quite immediate (max a few years) after or even during the eruption. The syn-eruptive features of these deposits are also testified by the absence of anthropic traces or humified surfaces within the deposits, as further evidence of a very short-term time span between the eruptions and the lahar events. Other interesting features are the presence of multiple depositional flow units evidenced by clast alignments and concave erosion surface inside the lahar deposits. Such flow units were emplaced by en-masse deposition (with reference to each flow pulse), and this can be argued by the generally massive facies of each flow unit in the deposits, and by the presence of water escape structures that cross vertically the entire lahar sequences. This latter evidence testifies a rapid and contemporaneous water loss through vertical escaping “pipes” soon after the emplacement of the sequence.

The analysis of the Pollena lithofacies allowed the identification of mainly two deposit categories. The first one occurs over an area that extends for more than 10 km north of Mount Somma, the second one occurs on an area which extends west of the Apennines. For the latter, we can recognize two significant sub-categories of deposits, corresponding to the main valleys in northwest-southeast direction, Avella-Baiano Valley and Lauro Valley. This difference seems to reflect the type of primary deposits that was remobilized and (just fine ash vs. ash and lapilli). In the first area, which comprises the municipalities of Acerra and Afragola, the primary lapilli fallout deposit is in fact not

https://doi.org/10.5194/egusphere-2023-1302
Preprint. Discussion started: 1 August 2023

deposited, while there is almost always a very thin level of phreatomagmatic ash in the Plain and thick, fine-grained pyroclastic current deposits in the Mt. Somma valleys feeding the lahars. The other basin comprises many municipalities in the area around Nola (Fig. 1 and Appendix 3), where the lahar deposits are generally coarser, and consist of multiple depositional units with different lithofacies. In this case both granulometry and componentry indicate the deposit resulted from the remobilization of the fallout deposit. A volume estimation of the remobilized syn-eruptive deposits, based on a GIS calculation, is of 73×10^6 m^3 for the northern Vesuvius area and 42×10^6 m^3 for the Lauro Valley.

Referring to the 1631 eruption, previous maps have shown the distribution of the 1631 lahar deposits toward east, basically following the distribution of the primary pyroclastic fall deposits (Sulpizio et al., 2006), while in Figs. 9 and 10 we show a significantly larger distribution area particularly toward north (Somma-Vesuvius ramps and Plain) and east (mountain valleys), and less toward the SE. In particular, this distribution is well explained by the wide distribution of the ash fallout deposit toward both north and northeast (Fig. 6), remobilized during the lahar generation along both Somma and Apennine slopes. On the other hand, looking at the deposit thicknesses, they reach on average half a meter to the N and NE, while reaching a couple of meters in some points to the NE (aligned with the dispersion axis of the primary fallout deposits and out of the Apennine valleys).

The sedimentological analyses carried out on a number of samples from the different studied sectors (Somma-Vesuvius, Lauro Valley, Avella-Baiano Valley) are useful for discriminating the various factors that contributed to emplace the lahar deposits. The samples for Lauro Valley and Avella-Baiano Valley are coarser (but have a significant finer tail) than the ones for Somma-Vesuvius, and this can depend on three factors: i) depositional mechanisms of the primary pyroclastic deposits (fall vs. flow); ii) interaction between lahars and morphology (valley vs. plain); iii) major involvement for Lauro Valley and Avella-Baiano Valley of the distal fine phreatomagmatic ash deposits formed in the final eruptions stages. In other words, the primary grain sizes involved in the remobilization (finer

https://doi.org/10.5194/egusphere-2023-1302
Preprint. Discussion started: 1 August 2023

and higher-water retention for Somma-Vesuvius), as well as the general topography (gentler but longer ramp for Somma-Vesuvius) likely acted as the main factors directly impacting the distribution of the lahar deposits, and the decay of the flow velocities and dynamic pressures in the area. Interestingly, an emplacement temperature (~120 °C) of the lahar deposits was calculated for those generated along the Somma-Vesuvius slopes, indicating a relatively hot provenance after remobilization of the pyroclastic current deposits. Instead, the remobilization from the Apennines sectors involved only cold fallout deposits. The paleomagnetic data of flow direction also indicate that the lahar emplacement at Nola and Acerra was not synchronous, as further evidence of the different timing and detachment areas involved during the pyroclasts remobilization. The parental lahars acted as mass flows capable of entraining outsized clasts (where available) from substrate under the action of flow dynamic pressure, then emplaced massive flow units with uplifted external clasts set into the much finer matrix. In various lahar units, multiple clasts have been found, showing some alignment that depends on the mechanisms of entrainment and uplift (with respect to substrate) within the flow.

In terms of local impact in the Pollena case study (the largest one), while most of the calculated points (44) fall in the range of lahar velocity of 2-4 m/s and dynamic pressure of 4-8 kPa, a few peak values of velocity of 13-15 m/s and dynamic pressure of 90-115 kPa are also calculated, which are directly related to meter-sized clasts entrained into the lahars on the steep slopes, then deposited downstream of alluvial fans. Such values of the velocity and dynamic pressure are well comparable with those calculated for lahars that occurred recently at Ruapehu in 2007 (Lube et al., 2012) and Merapi in 2011 (Jenkins et al., 2015), and in historical times at El Misti (Thouret et al., 2022). In particular, the estimated velocities and pressure agree with those of Lube et al. (2012) and Jenkins et al. (2015). Moreover, multiplying velocity and density gives a power per unit surface, so those most representative values correspond to a flow power per unit surface of $8\cdot10^3$ - $3.2\cdot10^4$ W/m^2, with peak values of $1.17\cdot10^6$ - $1.72\cdot10^6$ W/m^2, in agreement with typical values reported for floods and megafloods (Russell and Knudsen, 1999; Whipple et al., 2000; Carling, 2013).

https://doi.org/10.5194/egusphere-2023-1302
Preprint. Discussion started: 1 August 2023

6. Conclusions

A number of points can be highlighted after the integration of the historical, stratigraphic, sedimentological, laboratory, and impact parameter analyses carried out in the Vesuvius area for the Pollena and 1631 eruptions. In general, the physical characteristics of the analyzed deposits indicate that syn-eruptive lahars are related to the rapid remobilization of large volumes of pyroclastic material, which is mainly fine-grained and almost exclusively derived from the accumulation of products related to a single eruption. The analysis also shows that tardive (post-eruptive) mass flows are common, and involve multiple and variably altered deposits, and that their energy and frequency are progressively lower over time, after the last eruption has occurred. In particular, a higher impact both from primary and secondary phenomena is something that should be accounted in the Vesuvius area and that,

i) The new isopach maps of the Pollena and 1631 eruptions allow us to infer a larger impact than previously known for these two sub-Plinian events of the Vesuvius. Thus, it is worth reconsidering the territorial impact that sub-Plinian eruptions can have in the Vesuvius (but not only) area. In particular, the ash deposits can have a high impact in relation to their high density and low permeability.

ii) The primary impact from fallout and pyroclastic current processes in the Vesuvius area was - and may be in the future – followed by the secondary impact from lahars generated during or immediately after the eruption events. Both impacts can have a wide distribution, because they are directly controlled by the primary deposits distributions, both around Somma-Vesuvius and in the Apennines valleys.

iii) The runouts of such lahars were significant both for the Pollena and 1631 eruptions, by reaching distances of 10 to 15 km from the sources, and their deposits geometry is tabular-like with average thicknesses of 0.5 to 1 m.

https://doi.org/10.5194/egusphere-2023-1302
Preprint. Discussion started: 1 August 2023

iv) The paleotemperature data highlight a relatively hot dynamics (~120 °C) for those lahar flow pulses that traveled along the Somma-Vesuvius slopes because of pyroclastic current deposit remobilization. This did not occur from the Apennines sectors, where only cold fallout deposits were remobilized.

v) A reverse engineering approach allowed to calculate the local lahar velocities (2-4 m/s, with peaks of 13-15 m/s), dynamic pressures (4-8 kPa, with peaks of 90-115 kPa), and solid volumetric concentration (~30%, implying a 1:3 ratio between deposit and flow thickness), on the basis of the external clast properties entrained into the flows then emplaced into the ash matrix, and on the presence of the lahar deposits in proximity of obstacles and archaeological findings.

As a general conclusion, we have demonstrated that the areal impact of both primary deposits and lahars, in case of sub-Plinian events at Somma-Vesuvius, involves a territory wider than previously known and for several years, with possible decreasing damages over time.

Appendix A. Calculation of lahar velocities and dynamic pressures

A theoretical scheme is presented to quantify local dynamic pressures of the lahars, by inverting the field features at selected locations. The final goal is to map the values of dynamic pressure to assessing the hazard from lahars in the study area. Flow dynamic pressure, P_{dyn}, results from a combination of flow density, ρ_f, and flow velocity, v, and is defined as follows

$$P_{dyn} = 0.5\rho_f v^2 \quad \text{(A1)}$$

In the study area, the original flow was a multiphase flow of water + pyroclastic sediment, which during remobilization evolved into a flow of water + pyroclastic sediment + external clasts. Generically, flow density results from a combination of particle density, ρ_p, and water density, ρ_w, through particle volume concentration, C, and is defined as follows

https://doi.org/10.5194/egusphere-2023-1302
Preprint. Discussion started: 1 August 2023

$$\rho_f = \rho_p C + \rho_w (1 - C) \tag{A2}$$

In order to define flow velocity, we take into account stratigraphic and sedimentological characteristics of the lahar deposits: i) they are ubiquitously massive, and result from remobilization of the primary pyroclastic deposits then emplacement from mass flows; ii) they contain big external clasts entrained and uplifted from substrate into the flows. With these field characteristics, flow velocity can be expressed as a combination of entrained clast properties and flow density, and is defined as follows (modified after Roche, 2015)

$$v = \sqrt{\frac{X\psi(\rho_c - \rho_w)g}{\gamma\rho_f}} \tag{A3}$$

where X is clast small axis, Ψ is clast shape factor, ρ_c is clast density, g is gravity acceleration and γ is an empirical constant. Eq. 3 allows quantifying the incipient motion of the big clasts, and gives minimum values of flow velocity required to entrain and uplift the clasts from substrate, possibly more than once, before being emplaced into the lahar deposits. Such equation has been originally derived in laboratory experiments for a multiphase flow of air + sediment, and is highly performing at ρ_f ~ 1000 kg/m^3 (hindered settling) for dense pyroclastic currents controlled by topography then opened to alluvial plain (Martí et al., 2019), which is a case similar to the lahars in the study area. Substituting Eq. 3 into Eq. 1 and simplifying gives

$$P_{dyn} = 0.5\frac{X\psi(\rho_c - \rho_w)g}{\gamma} \tag{A4}$$

For given clast properties, flow dynamic pressure has a unique value, while flow velocity is a function of flow density. Indeed, the present scheme is a spot model that basically depends on, and is limited to, the finding of big clasts and boulders within the lahar deposits.

At the selected locations in the study area, we collected the dimensions of the biggest clasts found in the lahar deposits, and we characterized petrographically the clasts in the field, to calculate flow dynamic pressures using Eq. 4. We used the following values for the various parameters in the

https://doi.org/10.5194/egusphere-2023-1302
Preprint. Discussion started: 1 August 2023

calculations: Ψ (ellipsoid) = 0.66; ρ_c (limestone) = 2500 kg/m^3; ρ_c (ceramic) = 2000 kg/m^3; ρ_c (brick) = 2000 kg/m^3; ρ_c (tephra) = 1500 kg/m^3; ρ_c (lava) = 2500 kg/m^3; ρ_c (iron) = 8000 kg/m^3; ρ_w = 1000 kg/m^3; g = 9.81 m/s^2; γ = 0.031 – 0.071. Also, we calculated flow velocities using Eq. 3, in the following range of flow density: $\rho_w \leq \rho_f \leq \rho_p$, where ρ_w = 1000 kg/m^3 and ρ_p = 2000 kg/m^3. In this way, flow density spans from two extreme cases: i) $\rho_f = \rho_w$, negligible pyroclastic sediment and external clasts, so water flow only; ii) $\rho_f = \rho_p$, negligible water and dominant pyroclastic sediment, so ash flow only. For the empirical constant in Eq. 3, we used three different values to test the sensitivity with respect to different physical states of the multiphase flow: γ (non-fluidized) = 0.031; γ (initially fluidized and slightly expanded) = 0.057; γ (initially fluidized and non-expanded) = 0.071 (see Roche et al., 2013; Fig. A1).

Regarding flow velocity, after calculation we can rewrite Eq. 3 in a simpler form (to more directly relate velocity to density) as follows

$$v = \frac{a}{\sqrt{\rho_f}} \tag{A5}$$

where $a > 0$ depends on clast properties, and its square has dimension of pressure. On the other hand, it is not straightforward to constrain local flow velocities with unique values of flow densities, mostly because small variations of velocity correspond to large variations of density, and this is particularly valid for volcaniclastic mass flows (Carling, 2013; Jenkins et al., 2015; Roche, 2015; Martí et al., 2019; Guzman et al., 2020; Thouret et al., 2022).

https://doi.org/10.5194/egusphere-2023-1302
Preprint. Discussion started: 1 August 2023

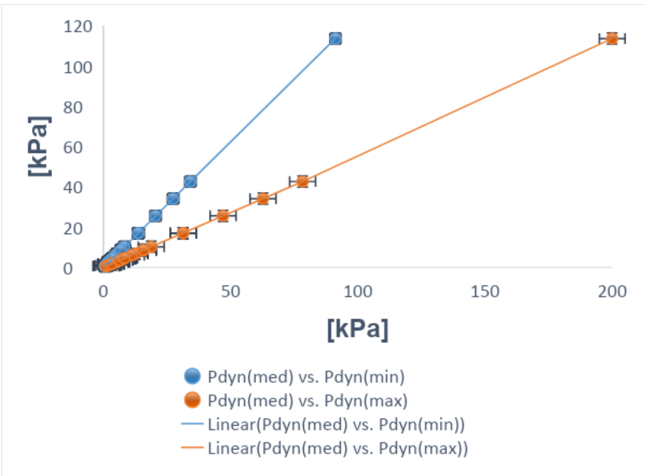

A

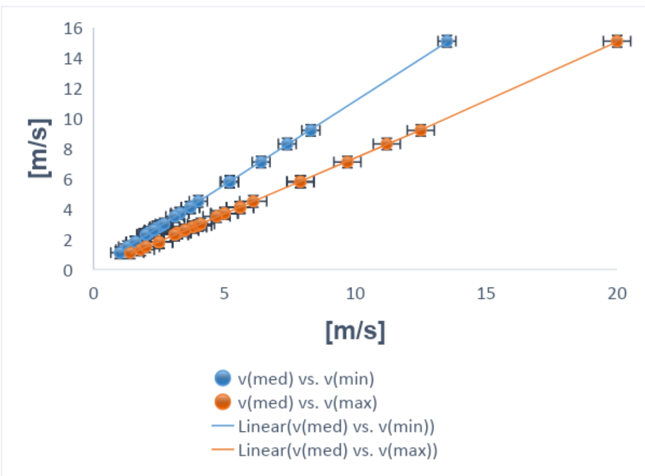

B

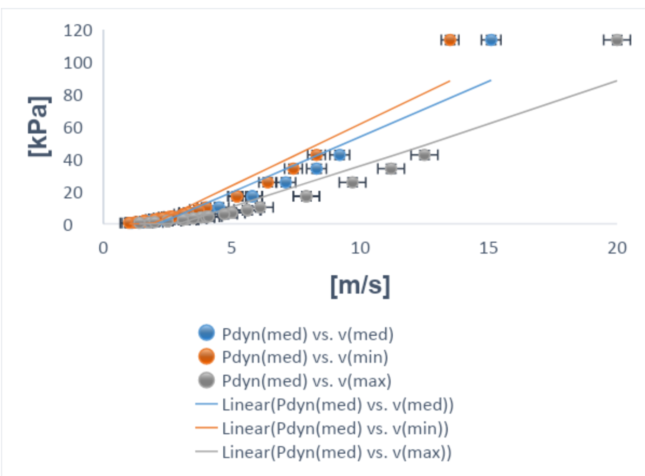

C

https://doi.org/10.5194/egusphere-2023-1302
Preprint. Discussion started: 1 August 2023

Fig. A1. **A**, dynamic pressure for the initially-fluidized and slightly expanded case vs. dynamic pressure for the initially-fluidized and non-expanded (blue) and non-fluidized (orange) cases; **B**, velocity for the initially-fluidized and slightly expanded case vs. velocity for the initially-fluidized and non-expanded (blue) and non-fluidized (orange) cases; **C**, dynamic pressure for the initially-fluidized and slightly expanded case vs. velocity for the initially-fluidized and slightly expanded (blue), vs. velocity for the initially-fluidized and non-expanded (orange), vs. velocity for the non-fluidized (grey) cases.

At some locations in the study area, we found lahar deposits against meter-scale manufacturing obstacles (Di Vito et al., 2009). The peculiarity is that the deposits in proximity of the obstacles are thicker than the correlated ones in the free field, but never reach the top of the obstacles themselves. This means that the lahars were not much expanded, so unable to overcome the obstacles as stratified flows would have done (cf. Spence et al., 2004; Gurioli et al., 2005; Doronzo, 2013; Breard et al., 2015). With this field evidence, we can assume that local flow height, H, was similar to deposit thickness against the obstacle, h_o, as follows

$$H \approx h_o \tag{A6}$$

In order to estimate flow density using Eq. 2, we focus on particle volumetric concentration. For well-sorted deposits, such concentration can be defined with an average value over flow height as follows (modified after Doronzo and Dellino, 2013; see also Eq. 30 in de' Michieli Vitturi et al., submitted)

$$C = \frac{h_f}{H} \tag{A7}$$

where h_f is deposit thickness in the free field. Substituting Eq. 6 into Eq. 7 gives

$$C \approx \frac{h_f}{h_o} \tag{A8}$$

In particular, h_f refers to those lahar deposits relatively close to the obstacles, but which were not affected by them during emplacement, i.e. close but not so much. We assessed that correlation taking into account the stratigraphic and sedimentological characteristics of the lahar deposits, and the fact

https://doi.org/10.5194/egusphere-2023-1302
Preprint. Discussion started: 1 August 2023

that Eq. 7 performs better with layers emplaced after remobilization of primary pyroclastic fallout or dominantly ash flow deposits.

Lastly, we macroscopically assessed erosion in the field, by characterizing the unconformities present both on the primary pyroclastic and lahar deposits. In particular, the syn-eruptive lahar deposits consist of more than one flow unit, so it is important to understand how the different flow pulses interacted with each other during emplacement. The main unconformities that are found in the field are referred to the partial absence of a flow unit, and the loss of lateral continuity despite some flat geometry of the deposits. On the other hand, at some locations we were not able to assess if erosion occurred or not due to multiple open issues: i) eventual absence of the primary pyroclastic deposits; ii) eventual exclusive presence of the post-eruptive lahar deposits; iii) impossibility to get to some outcropping deposit base and eventual unconformities.

Appendix B. Paleo-temperature and paleo-direction determinations

The magnetic fabric of a deposit was investigated by measurements of the magnetic susceptibility and its anisotropy (AMS). AMS was measured with a Kappabridge KLY-3 (AGICO), and data were elaborated by the software Anisoft5 (AGICO). AMS depends on the type, concentration, and distribution of all the minerals within the specimen. It is geometrically described by a triaxial ellipsoid, whose axes coincide with the maximum (k_1), intermediate (k_2) and minimum (k_3) susceptibility directions. The magnetic fabric of a specimen is then described by the direction of the k_1 axis, the magnetic lineation (L) and that of the k_3 axis, which is parallel to the pole of the magnetic foliation plane (F). Besides, the modulus of the susceptibility axes provides some magnetic parameters useful to express the intensity of the anisotropy (P_j) and the oblate/prolate fabric occurrence (T) (Jelinek, 1981). Generally, sedimentary vs pyroclastic deposits fabric, here considered as the proxy of the lahar fabric, is oblate with a horizontal to gently imbricated (less than 20°) magnetic foliation. The magnetic lineation is normally clustered along the foliation plunge. In this

https://doi.org/10.5194/egusphere-2023-1302
Preprint. Discussion started: 1 August 2023

case, both the F imbrication and the L direction can provide the local flow direction. Other times, L is orthogonal to the F plunge or F is statistically horizontal, and it is not possible to infer the flow direction.

For T_{dep} estimation, pottery sherds were subjected to progressive thermal demagnetization (PTD), with heating steps of 40 °C, up to the Curie Temperature (T_C), using the Schonstedt furnace and the spinner magnetometer JR6 (AGICO). The rationale of the method has been described in detail in several papers (McClelland and Druitt, 1989; Bardot, 2000, Porreca, 2007; Paterson et al., 2010; Lesti et al., 2011), many of them dedicated to PDCs of the Vesuvian area (Cioni et al., 2004; Di Vito et al., 2009; Giordano et al., 2018; Zanella et al., 2007; 2018; 2015). Typically, measurements are made on accidental lava lithics that were entrained during pyroclastic or lahar flows. In this case, we had the opportunity to estimate the T_{dep} by measuring ancient pottery artifacts. Briefly, pottery is characterized by a thermal remanent magnetization (TRM) acquired during its manufacture and its subsequent history of daily use. Whenever it is heated, part of its TRM, the one associated with blocking temperatures (T_b) below the heating one (T_h), is overwritten. Without alteration phenomena, the heating/cooling is a reversible process, except for the magnetic directions. The original TRM shows a random paleomagnetic direction, due to the transport during emplacement. Subsequent TRMs show directions parallel to the Earth's magnetic field during their cooling. This is clearly illustrated in the Zijderveld diagrams. The composition of the different magnetization components reveals thermal intervals characteristic of the heating history of the potsherd. Of course, this explanation is simplified, but the method is well-established and has been shown to work well with heated artifacts, such in the case of tiles and pottery embedded in the PDC deposits at Pompeii (Gurioli et al., 2005; Zanella et al.,2007), Afragola (Di Vito et al., 2009) and Santorini (Tema et al., 2015). In case of lahar, we expect low T_{dep} or cold deposits. This can be a major concern because of the difficulties to distinguish between the TRM secondary components, and the chemical (CRM) and viscous (VRM) remanent magnetization. The CRM may develop due to mineralogical changes during reheating (McClelland, 1996). Instead, VRM is typical of ferromagnetic grains with low T_b and often

https://doi.org/10.5194/egusphere-2023-1302
Preprint. Discussion started: 1 August 2023

occurs in most rocks. Following Bardot and McClelland (2000) relationship for time intervals in the 10^2–10^6 year range, T_b=75+15 log (acquisition time in years), and using the Pollena eruption date (472 AD), e obtain a lower limit of the T_b around 123 °C. This means that this temperature helps us in discriminating between "hot" (T_b > 120 °C) or "cold" lahar (Tb < 120 °C).

Finally, routine magnetic measurements on the lahar matrix were done on the lahar matrix to determine the Characteristic Remanent Magnetization (ChRM) by Thermal and Alternating Field demagnetizations. The direction of the Earth's Magnetic Field during the Pollena eruption is well-known (Zanella et al., 2008). If the sampled lahars were emplaced shortly after the eruption, both the secondary TRMs and the matrix of the lahars should show a remanent magnetization direction similar to the Pollena ones. ChRMs can also test if the two lahars (Acerra and Nola) are coeval.

Appendix C. Description of the studied areas

Area 1 – Nola

In the area surrounding Nola, it is possible to recognize the complete fallout sequence of the Pollena eruption (a in fig. C1 and C2), which usually covers ploughed soils (p in fig C1) and late Roman archaeological remains. The sequence is composed by an alternation of coarse pumice and thin ash fallout layers. Its top is always made of a cohesive ash bed related to the phreatomagmatic phase of the eruption (b in fig. C1 and C2), with a thickness ranging from 1 to 14 cm due to erosion. They are almost always overlain by lahar deposits composed of several flow units (c in fig. C1 and C2) with a large thickness variability due to channeling and presence of barriers and edifices. They sometimes include blocks, tiles, and other archaeological remains.

In Fig. C1, above the primary deposit, there is an example of a well-exposed sequence composed by at least five units (c in fig. C1). The first one is a massive and matrix-supported deposit composed by fine and not vesiculated ash (lithofacies Gms), with fragments of greenish to blackish scoriae and minor fragments of pumices, lavas and limestones. The fragments are cm-sized and are both angular

https://doi.org/10.5194/egusphere-2023-1302
Preprint. Discussion started: 1 August 2023

and rounded. The second flow unit is similar to the one below, but is darker and contains less coarse fragments. Its matrix is composed by an alternation of fine to medium ash. It follows a plane-parallel sequence of well-sorted fine sand and silt layers characterized by the lithofacies fM. A massive deposit follows upward, it is progressively humified and contains abundant reworked and rounded pumices from the Avellino eruption. The top humified surface is almost always eroded by anthropogenic activity and is generally ploughed (p1 in Fig. C1), whose surface is overlain by the primary deposits of the eruption of 1631 (d in Fig. C2). It is few cm thick and is composed by a basal layer of dark coarse ash (small pumice fragments), overlain by a very cohesive and massive ash bed, containing abundant accretionary lapilli. The following deposit thickens in the plowing furrows and depressions, and is composed by massive fine-ash beds, vesiculated and cohesive, and is interpreted as a lahar deposit (lithofacies mM) (e in Fig. C2). This deposit (e in Fig. C3) overlies the foundations of Palazzo Orsini (blocks in Fig. C3), now seat of the Court of Nola and built in the second half of the XV century (Fig. C3). The top is always eroded by the modern anthropogenic activity, and locally by deposits of recent eruptions of Vesuvius (e.g., 1822, 1906).

https://doi.org/10.5194/egusphere-2023-1302
Preprint. Discussion started: 1 August 2023

Fig. C1. Nola, Pollena fallout deposits overlain by at least five lahar units.

https://doi.org/10.5194/egusphere-2023-1302
Preprint. Discussion started: 1 August 2023

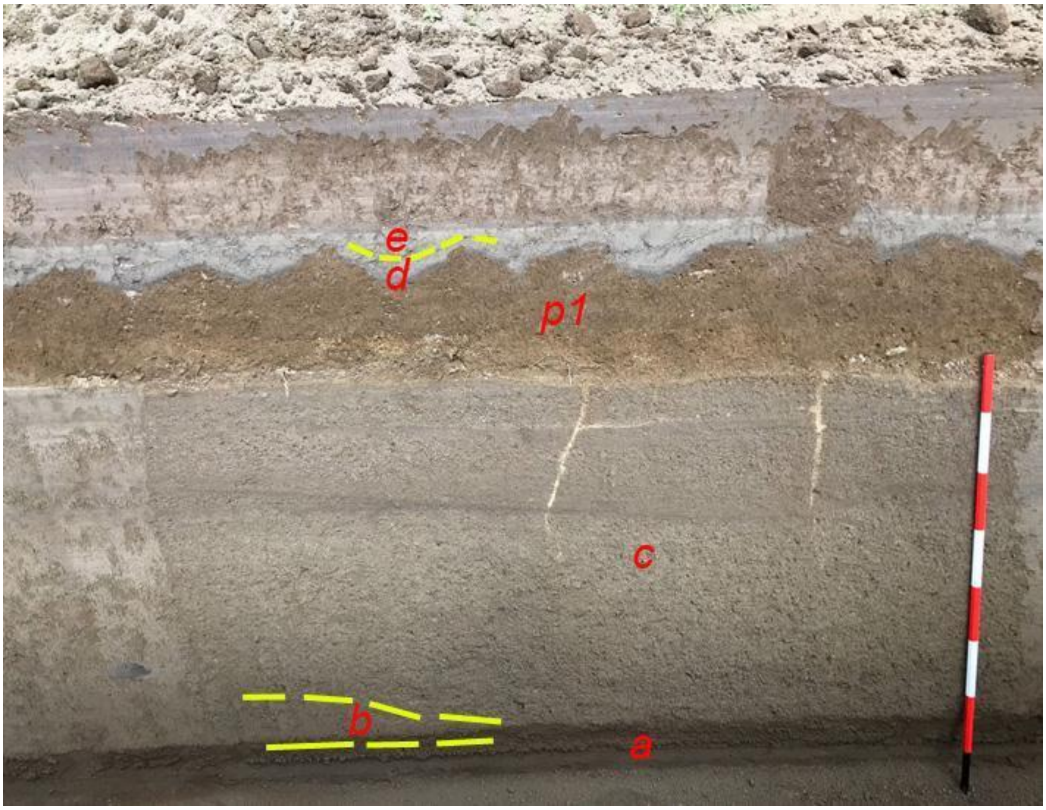

Fig. C2. Pollena lahar deposits overlain by a cultivated paleosoil and by the 1631 ash fallout and lahars.

https://doi.org/10.5194/egusphere-2023-1302
Preprint. Discussion started: 1 August 2023

Fig. C3. Palazzo Orsini, Nola (1631 fallout and lahars).

In Nola and in the nearby Cimitile, the effects on the territory of the lahar emplacement related to the Pollena eruption are testified by numerous archaeological remains. The Nola and Cimitile areas are covered by thick sequences of fallout and lahar deposits. In fact, the previous ground level was at least 2-3 m below the present one. This effect is well visible in the Amphitheater Laterizio, which was completely filled by the primary and secondary deposits, and the same in Cimitile, where in the

https://doi.org/10.5194/egusphere-2023-1302
Preprint. Discussion started: 1 August 2023

archaeological site of the Early Christian basilicas the present ground level is about two meters higher than the one before the eruption. It is worth noting that in Cimitile the flows were able to carry limestone blocks of 50 cm in diameter, likely along the main flow direction of the lahars (Fig. C4).

Fig. C4. Cimitile. Sequence of three m-thick lahar units with evidences transport of calcareous block (up to 50 cm). The largest are in the lower unit.

Area 2 – Acerra-Afragola

The Acerra and Afragola territories are located north and north-west of Vesuvius, and are almost flat areas crossed by the Clanis river. Both the coarse fallout deposits of the Pollena and 1631 eruptions are absent in this area. Here, only a thin, centimetric ash bed overlies the Late Roman paleosoil. This ash bed, which we correlate with the final phreatomagmatic phases of the Pollena eruption, is homogeneous, cohesive and mantles the ground without any significant lateral variation. The overlying deposit is characterized by high thickness variations, is generally massive and contains

https://doi.org/10.5194/egusphere-2023-1302
Preprint. Discussion started: 1 August 2023

vesicles from circular to flattened and coated by fine ash. It has a matrix-supported texture and is composed of fine to very fine, very cohesive ash, and contains scattered and more or less abundant pumice and lithic fragments (lithofacies mM) and remains of vegetation (Barone et al., 2023). From one to three depositional units have been recognized, marked by unconformities, and differences in grain-size or color. The uppermost unit always contains white pumice fragments of the Avellino eruption. Very common are drying out structures and water escape structures, which are vertical structures (Fig. C5), like fractures a few cm large, filled by finer material transported by the escaping water, formed soon after the emplacement of the syn-eruptive lahars (Fig. C5). The maximum thickness recorded in this area is about 90 cm.

Fig. C5. Lahar deposit (unit 2) in Acerra overlaying a cultivated paleosoil (unit 3). The index finger indicates a water escape structure.

https://doi.org/10.5194/egusphere-2023-1302
Preprint. Discussion started: 1 August 2023

The top is almost always horizontal due to the erosion related to the modern anthropogenic activity, and only in a few exposures it is capped by a paleosoil, with traces of human presence of the Medieval times and of the deposits of the 1631 eruption as well. The base of this latter deposit is a cm-thick fine-ash bed with an internal plane-parallel layering emplaced by fallout. It underlies a massive deposit with high thickness variations (max 20 cm) at the outcrop scale, is composed by fine ash, cohesive and vesiculated and contains scattered small pumice fragments (lithofacies mM). The pumice fragments are vesicular, dark gray to blackish, highly porphyritic with leucite, pyroxene and feldspar crystals. The stratigraphic position and lithology confirm their attribution to the 1631 primary and secondary (lahars) deposits.

Area 3 – Pomigliano-Marigliano

This area is located along the northern outer part of the Vesuvius apron (Santacroce et al., 2003). The studied sequences start from the paleosoil developed on top of ash the deposits of the AD 79 eruption. The paleosoil is mature and contains pottery fragments till the II century AD. Its top is undulated with traces of ploughing spaced about 50 cm (a in Fig. C6). Representative sequences of the area include a basal ash layer with a thickness ranging from 1 to 4 cm (b in Fig. C7), thickening in the depressions, cohesive and locally vesiculated. It is here interpreted as co-ignimbritic ash emplaced by fallout during the phreatomagmatic final phases of the Pollena eruption. Upwardly, the sequence includes several lahar units from massive to slightly stratified, composed by fine and very cohesive ash, and containing scattered greenish pumice fragments (lithofacies mM) (b1 in Fig. C7). Locally this deposit, also in the case of multiple units, is cut by vertical drying cracks. The sequence is overlain by a 25-30 cm thick mature paleosoil, containing cultivation traces and majolica fragments (c in Figs. C6 and C7).

The top of this paleosoil is undulated and covered by the primary deposit of the 1631 eruption (d in Fig. C7). This latter is represented by a discontinuous medium to fine ash layer, slightly laminated for contrasting grain size, up to 5 cm thick, with a gray to violet color, and containing dark pumice

https://doi.org/10.5194/egusphere-2023-1302
Preprint. Discussion started: 1 August 2023

fragments and loose crystals of leucite, pyroxene and biotite (Fig. C7). Its thickness variation is due both to slight internal variations (thickening in correspondence of depressions) and erosion by the following lahars. These latter are composed of one to three flow units (d1 in Fig. C7), with a cumulative total thickness varying from 10 to 45 cm. They are composed of massive fine and very cohesive ash, and contain rare scattered dark pumice fragments similar to those of the 1631 eruption (lithofacies mM). These sequences are overlain by recent, cultivated soil. Locally, thin ash beds of the recent Vesuvius activity (like 1822, 1906) overlie the 1631 deposits.

Fig. C6. Pomigliano locality. Sequence of deposits including bottom to top: Bronze Age paleosoil, Pomici di Avellino (unit EU 5 of Di Vito et al., 2009), paleosoil developed on top of Pomici di Avellino and buried by the Pollena eruption deposits. In the central part, fine ash deposits of the 79 CE eruption are visible. The top of the paleosoil is undulated and ploughed. a,b) primary and secondary deposits of the Pollena eruption, c) paleosoil between Pollena and 1631 deposits, d) 1631 primary and secondary deposits..

https://doi.org/10.5194/egusphere-2023-1302
Preprint. Discussion started: 1 August 2023

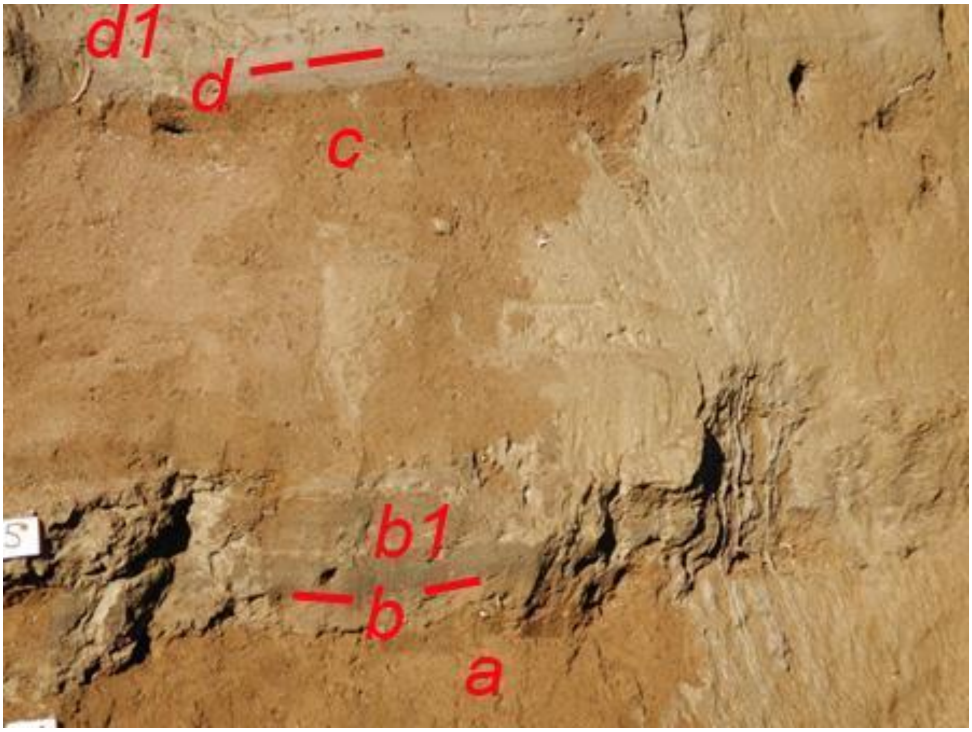

Fig. C7. Particular of the Fig. C6. a) paleosoil containing potteries of the II Cent. AD; b) ash deposit of the Pollena eruption; b1) syn-eruptive lahars of the Pollena eruption; c) paleosoil between Pollena and 1631; d) primary deposits of the 1631 eruption, overlain by syn-eruptive lahars (d1).

Area 4 – Avella-Baiano valley

We have analyzed several sequences along the *Avella-Baiano* valley, both exposed and excavated for the present work. Here the sequences of primary deposits are often affected by deep erosion, in fact, in some places the Pollena primary deposits are completely lacking and only the syn-eruptive lahar deposits are present on top of the late Roman paleosoil. Where preserved, the paleosoil has often an undulated surface due to cultivation (ploughing and hoeing). The Pollena eruption sequence consists of an alternation of coarse pumice and fine ash layers emplaced by fallout (a in Fig. C8). It is up to 50 cm thick and ends with a cohesive yellowish ash layer (b in Fig. C8), overlain by the lahar deposits, generally composed by 2-3 flow units (c in Fig. C8). The total thickness of the lahars is largely

https://doi.org/10.5194/egusphere-2023-1302
Preprint. Discussion started: 1 August 2023

variable with maxima at the base of the slopes where it can reach 2-3 m. In some excavations we did not reach the base of the deposit, deeper than 3.5 m. In Fig. C8, it is possible to observe a complete sequence of deposits of Pollena overlying a late Roman paleosoil. The sequence includes the fallout layers and thick lahar deposits. These latter are always massive, matrix-supported, and contain abundant scattered pumice and lithic fragments (lithofacies Gms). In some cases, the lower part contains several limestone fragments up to 10 cm in diameter. The described deposit has been also found in the Roman Amphitheatre of Avella, where it has a variable thickness (order of decimetric). Here, it has been almost all excavated and only remnants are presently exposed.

Generally, the upper part of the sequences is composed by an alternation of plane-parallel to cross-layered sands and gravels, with abundant rounded limestone fragments, emplaced by several alluvial episodes (post-eruptive) (lithofacies Sh-Ss). In these post-eruptive deposits, it is not uncommon to find terracotta fragments from the Imperial Roman age.

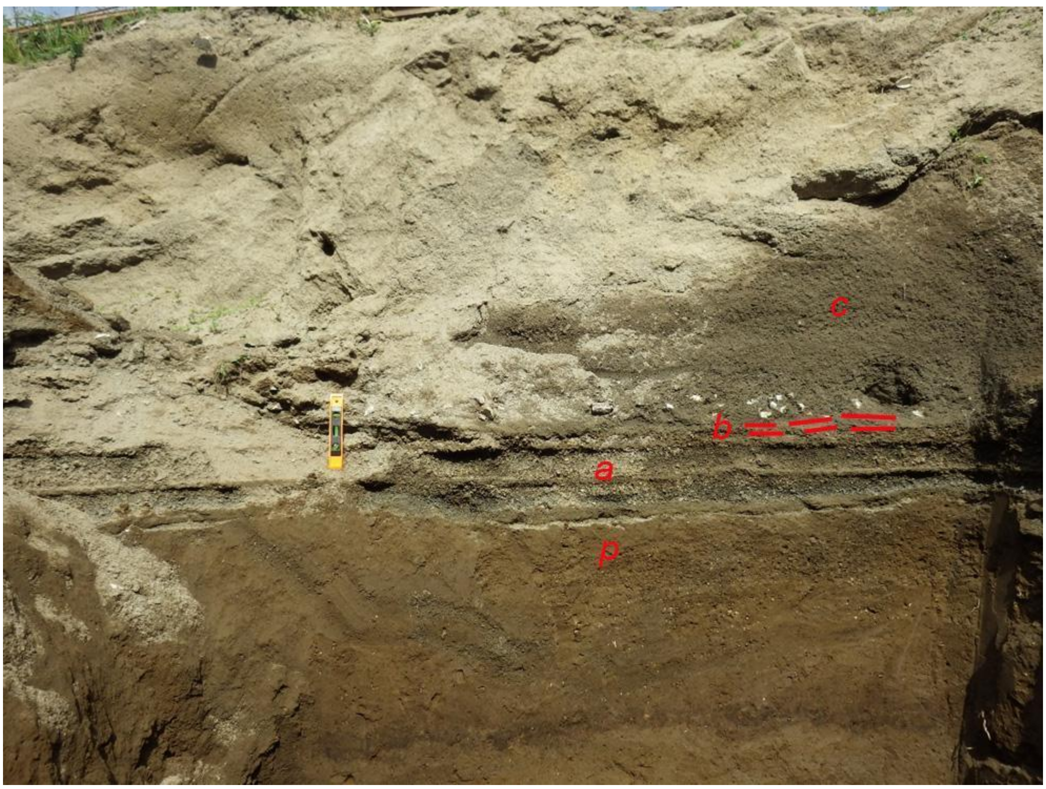

https://doi.org/10.5194/egusphere-2023-1302
Preprint. Discussion started: 1 August 2023

Fig. C8. Avella-Baiano ValleyAvella valley. The Pollena primary deposit (a,b) lies on a ploughed soil (p) and it is covered by at least three flow units of lahars.

The Pollena primary and secondary sequences are overlain by a mature paleosoil with frequent evidence of cultivation (ploughing, p in Fig. C9) and locally by the 1631 eruption deposits. The primary deposit related to the 1631 eruption is not always present. It is up to 2 cm (a in Fig. C9) thick ash layer, gray-violet in color deposited by fallout deposit and overlaying a ploughed paleosoil (p in Fig. C9). It is overlain by lahar deposits (b in Fig. C9) composed by several units and characterized by contrasting grain-sizes. The deposits are composed of medium ash, are massive and matrix-supported, and contain abundant scattered mm- to cm-sized pumice fragments (all with the same lithology of the primary deposits) and sometimes vegetal remain traces (lithofacies Gms).

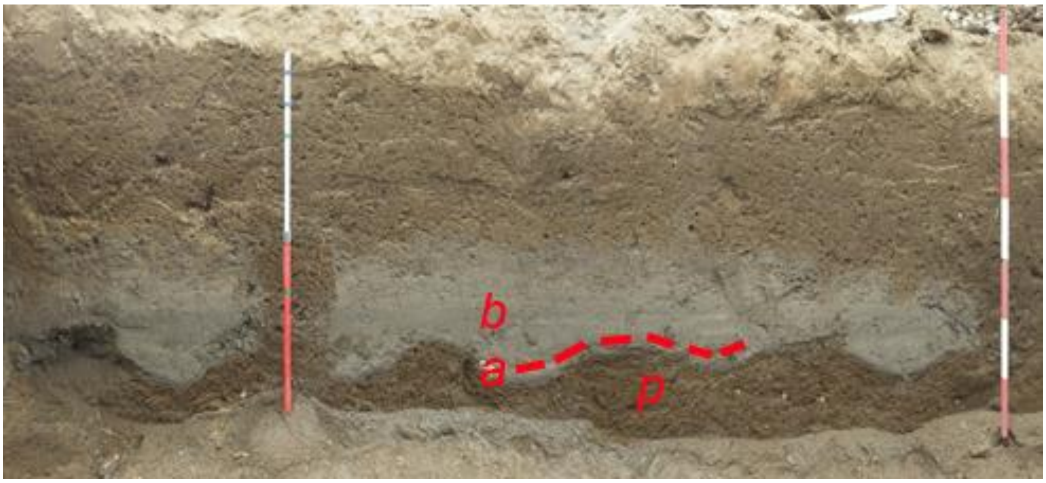

Fig. C9. Avella-Baiano ValleyAvella valley: particular of the 1631 primary (a) and secondary deposits (b, syn-eruptive lahars) in a trench at Cicciano locality.

Area 5 – Lauro ValleyVallo di Lauro

Lauro ValleyVallo di Lauro has characteristics similar to the Avella-Baiano ValleyAvella valley, but the primary deposits of Pollena and 1631 eruptions are thicker (Figs. 5 and 6) and coarser. In this valley also the sequences are locally deeply eroded. In fact, the deposits of the Pollena eruption

https://doi.org/10.5194/egusphere-2023-1302
Preprint. Discussion started: 1 August 2023

(normally 50-70 cm thick) (Fig. C10) are sometimes missing. They overlie a mature paleosoil with abundant traces of cultivation. Overall, the characteristics of the deposits are very similar to the ones of the Nola area. The overlying lahar deposits are always massive, matrix-supported, and composed of fine and very cohesive ash with abundant scattered pumices and lithic fragments (similar in lithology to those of the primary deposits) (lithofacies Gms). These deposits have a high variable thickness, with a measured maximum up to 2 m, but sometimes reduced by erosion. In some trenches the base of the sequences was deeper than the investigated depth (>3.5 m).

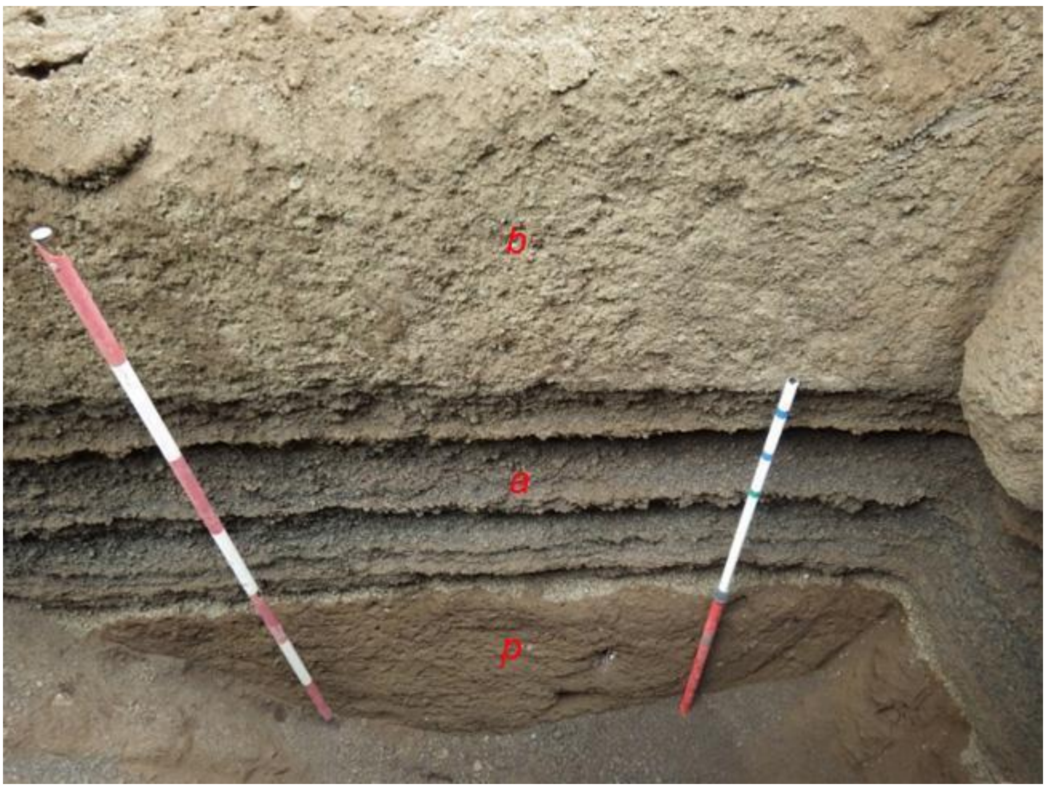

Fig. C10. Lauro valley, Pago del Lauro ValleyVallo di Lauro. Sequence of Pollena fallout deposits (a) overlain by syn-eruptive lahars (b). At the base the late Roman paleosoil (p).

https://doi.org/10.5194/egusphere-2023-1302
Preprint. Discussion started: 1 August 2023

It is possible to evaluate the effects of the lahars on building in the Roman Villa di Lauro, at Taurano, where a 70 cm thick fallout is overlain, without paleosoil, by syn-eruptive lahars which engulfed and transported pieces of walls, bricks and potteries. The lahar deposits are matrix supported and composed by fine to coarse ash and contain abundant pumice lapilli (all similar to the Pollena fallout deposits). They are massive, cohesive and have a thickness up to about 1 m, thickening in depressions and near barriers (Fig. C11).

The sequence related to the eruption of 1631 is not always present, but it is possible to find its primary deposit, composed by a basal layer of stratified fine and medium thin ash beds, and minor dark pumice and lithic fragments overlain by a thin, very fine and cohesive accretionary lapilli-rich ash bed. The maximum measured thickness is 30 cm. The overlying lahar deposits are massive and matrix-supported, composed of fine to coarse ash and contain abundant pumice fragments of the primary deposit.

https://doi.org/10.5194/egusphere-2023-1302
Preprint. Discussion started: 1 August 2023

Fig. C11. Taurano (Villa Lauro), baulk showing a thick sequence of lahar units filling the Roman Villa. Some units engulf and transport pieces of walls and large blocks.

Author contribution

MDV: conceptualization, investigation, methodology, writing - original draft preparation, writing - review & editing, funding acquisition; IR: data curation, investigation, writing - original draft preparation; SdV: investigation, writing - original draft preparation, writing - review & editing; DMD: investigation, methodology, data curation, writing - original draft preparation, writing - review & editing; MB: data curation, methodology, writing - original draft preparation; MdMV: writing - review & editing; MR: conceptualization, writing - review & editing; LS: writing - review & editing; GZ: investigation, writing - review & editing; EZ: investigation, methodology, writing - original draft preparation; AC: conceptualization, writing - review & editing, funding acquisition.

Acknowledgements

This work benefited of the agreement between Istituto Nazionale di Geofisica e Vulcanologia and the Italian Presidenza del Consiglio dei Ministri, Dipartimento della Protezione Civile (DPC), Convenzione B2. The paper does not necessarily represent DPC official opinion and policies.

References

Acocella V and Funiciello R (2006) Transverse systems along the extensional Tyrrhenian margin of Central Italy and their influence on volcanism. Tectonics 25,1-24.

https://doi.org/10.5194/egusphere-2023-1302
Preprint. Discussion started: 1 August 2023

Arguden AT and Rodolfo KS (1990) Sedimentologic and dynamic differences between hot and cold laharic debris flows of Mayon Volcano, Philippines. Geological Society of America Bulletin 102, 865-876.

Bardot L (2000) Emplacement temperature determinations of proximal pyroclastic deposits on Santorini, Greece, and their implications. Bulletin of Volcanology 61, 450-467.

Bardot L, McClelland E (2000) The reliability of emplacement temperature estimates using paleomagnetic methods: a case study from Santorini, Greece. Geophysical Journal International 143, 39-51.

Bartole R (1984) Tectonic Structure of the Latian-Campanian Shelf (Tyrrhenian Sea). Bollettino di Oceanologia Teorica Applicata 2, 197-230.

Bisson M, Pareschi MT, Zanchetta G, Sulpizio R, Santacroce R (2007) Volcaniclastic debris-flow occurrences in the Campania region (Southern Italy) and their relation to Holocene–Late Pleistocene pyroclastic fall deposits: implications for large-scale hazard mapping. Bulletin of Volcanology 70, 157-167.

Bisson M, Spinetti C, Sulpizio R (2014) Volcaniclastic flow hazard zonation in the Sub-Apennine Vesuvian area using GIS and remote sensing. Geosphere 10, 1419-1431.

Bisson M, Zanchetta G, Sulpizio R, Demi F (2013) A map for volcaniclastic debris flow hazards in Apennine areas surrounding the Vesuvius volcano (Italy). Journal of Maps 9, 230-238.

Blott SJ and Pye K (2001) Gradistat: A Grain Size Distribution and Statistics Package for the Analysis of Unconsolidated Sediments. Earth Surface Processes and Landforms 26, 1237-1248.

Braccini GC (1632) Dell’Incendio Fattosi nel Vesuvio a XVI di Dicembre MDCXXXI. Secondino Roncagliolo, 104 pp.

https://doi.org/10.5194/egusphere-2023-1302
Preprint. Discussion started: 1 August 2023

Brancaccio L, Cinque A, Romano P, Rosskopf C, Russo F, Santangelo N, Santo A (1991) Geomorphology and neotectonic evolution of a sector of the Tyrrhenian flank of the Southern Apennines (Region of Naples, Italy). Zeitschrift für Geomorphologie Supplement Bd. 82, 47-58.

Breard ECP, Lube G, Cronin SJ, Valentine GA (2015) Transport and deposition processes of the hydrothermal blast of the 6 August 2012 Te Maari eruption, Mt. Tongariro. Bulletin of Volcanology 77, 100.

Brocchini D, Principe C, Castradori D, Laurenzi MA, Gorla L (2001) Quaternary evolution of the southern sector of the Campanian Plain and early Somma-Vesuvius activity: insights from the Trecase 1 well. Mineralogy and Petrology 73, 67-91.

Carling PA (2013) Freshwater megaflood sedimentation: What can we learn about generic processes? Earth-Science Reviews 125, 87-113.

Carrara E, Iacobucci F, Pinna E, Rapolla A (1973) Gravity and magnetic survey of the Campanian volcanic area, S. Italy. Bollettino di Geofisica Teorica e Applicata 15, 39-51.

Cas RAF, Wright HMN, Folkes CB, Lesti C, Porreca M, Giordano G, Viramonte JG (2011) The flow dynamics of an extremely large volume pyroclastic flow, the 2.08-Ma Cerro Galán Ignimbrite, NW Argentina, and comparison with other flow types. Bulletin of Volcanology 73, 1583-1609.

Cinque A and Robustelli G (2009) Alluvial and coastal hazards caused by long-range effects of Plinian eruptions: The case of the Lattari Mts. After the AD 79 eruption of Vesuvius. Geological Society London Special Publications 322, 155-171.

Cioni R, Gurioli L, Lanza R, Zanella, E (2004) Temperatures of A.D. 79 pyroclastic density current deposits (Vesuvius, Italy). Journal of Geophysical Research 109, B02207.

Costa JE (1997) Hydraulic modeling for lahar hazards at Cascades volcanoes. Environmental Engineering Geoscience 3, 21-30.

D'Argenio B, Pescatore TS, Scandone P (1973) Schema geologico dell'Appennino meridionale (Campania e Lucania). In: Moderne vedute sulla geologia dell'Appennino. Convegno (Roma, 16-18 Febbraio 1972). Accademia Nazionale dei Lincei, Problemi Attuali di Scienza e Cultura, Quaderni 183, 49-72.

de' Michieli Vitturi M, Costa A, Di Vito MA, Sandri L, Doronzo DM (submitted). Lahar events in the last 2,000 years from Vesuvius eruptions. Part 2: Formulation and validation of a computational model based on a shallow layer approach.

De Simone GF, Perrotta A, Scarpati C (2011) L'eruzione del 472 d.C. ed il suo impatto su alcuni siti alle falde del Vesuvio. Rivista Studi Pompeiani 22, 61.71.

De Vivo B, Rolandi G, Gans PB, Calvert A, Bohrson WA, Spera FJ, Belkin HE (2001) New constraints on the pyroclastic eruptive history of the Campanian volcanic Plain (Italy). Mineralogy and Petrology 73, 47-65.

Di Crescenzo G and Santo A (2005) Nuovo contributo sul ruolo svolto dai livelli pomicei nelle aree di distacco delle frane di colata rapida dei massicci carbonatici campani. Convegno Nazionale La mitigazione del rischio da colate di fango a Sarno e negli altri Comuni colpiti dagli eventi del maggio 1998. Napoli, 2 e 3 maggio 2005 - Sarno 4 e 5 maggio 2005.

Di Vito MA, Castaldo N, de Vita S, Bishop J, Vecchio G (2013) Human colonization and volcanic activity in the eastern Campania Plain (Italy) between the Eneolithic and Late Roman periods. Quaternary International 303, 132-141.

Di Vito MA, Sulpizio R., Zanchetta G (1998). I depositi ghiaiosi della valle dei torrenti Clanio e Acqualonga (Campania centro-orientale): significato stratigrafico e ricostruzione paleoambientale. Il Quaternario Italian Journal of Quaternary Sciences 11, 273-286.

Di Vito MA, Talamo P, de Vita S, Rucco I, Zanchetta G, Cesarano M (2019) Dynamics and effects

https://doi.org/10.5194/egusphere-2023-1302
Preprint. Discussion started: 1 August 2023

of the Vesuvius Pomici di Avellino Plinian eruption and related phenomena on the Bronze Age landscape of Campania region (Southern Italy). Quaternary International 499, 231-244.

Di Vito M, Zanella E, Gurioli L, Lanza R, Sulpizio R, Bishop J, Tema E, Boenzi G, Laforgia E (2009) The Afragola settlement near Vesuvius, Italy: The destruction and abandonment of a Bronze Age village revealed by archeology, volcanology and rock-magnetism. Earth and Planetary Science Letters 277, 408-421.

Doronzo DM, Dellino P (2013) Hydraulics of subaqueous ash flows as deduced from their deposits: 2. Water entrainment, sedimentation, and deposition, with implications on pyroclastic density current deposit emplacement. Journal of Volcanology and Geothermal Research 258, 176-186.

Doronzo DM (2013) Aeromechanic analysis of pyroclastic density currents past a building. Bulletin of Volcanology 75, 684.

Duller RA, Mountney NP, Russell AJ, Cassidy NC (2008) Architectural analysis of a volcaniclastic jökulhlaup deposit, southern Iceland: sedimentary evidence for supercritical flow. Sedimentology 55, 939-964.

Faccenna C, Funiciello R, Bruni A, Mattei M, Sagnotti L (1994) Evolution of a transfer related basin: the Ardea basin (Latium, Central Italy). Basin Resources 5, 1-11.

Fedi M and Rapolla A (1987) The Campanian Volcanic Area: analysis of the magnetic and gravimetric anomalies. Bollettino della Società Geologica Italiana 106, 793-805.

Finetti I and Morelli C (1974) Esplorazione di sismica a riflessione nei Golfi di Napoli e Pozzuoli. Bollettino di Geofisica Teorica e Applicata 16, 62-63.

Fiorillo F and Wilson RC (2004) Rainfall induced debris flows in pyroclastic deposits, Campania (southern Italy). Engineering Geology 75, 263-289.

https://doi.org/10.5194/egusphere-2023-1302
Preprint. Discussion started: 1 August 2023

Giordano G, Zanella E, Trolese M, Baffioni C, Vona A, Caricchi C, De Benedetti AA, Corrado S, Romano C, Sulpizio R, Geshi N (2018) Thermal interactions of the AD79 Vesuvius pyroclastic density currents and their deposits at Villa dei Papiri (Herculaneum archaeological site, Italy). Earth and Planetary Science Letters 490, 180-192.

Girolami L, Roche O, Druitt T, Corpetti T (2010) Velocity fields and depositional processes in laboratory ash flows, with implications for the dynamics of dense pyroclastic flows. Bulletin of Volcanology 72, 747-759.

Gurioli L, Pareschi MT, Zanella E, Lanza R, Deluca E, Bisson M (2005) Interaction of pyroclastic density currents with human settlements: Evidence from ancient Pompeii. Geology 33, 441-444.

Gurioli L, Sulpizio R, Cioni R, Sbrana A, Santacroce R, Luperini W, Andronico D (2010) Pyroclastic flow hazard assessment at Somma-Vesuvius based on the geological record. Bulletin of Volcanology 72, 1021-1038.

Guzman S, Doronzo DM, Martí J, Seggiaro R (2020). Characteristics and emplacement mechanisms of the Coranzulí ignimbrites (Central Andes). Sedimentary Geology 405, 105699.

Ippolito F, Ortolani F, Russo M (1973) Struttura marginale tirrenica dell'Appennino campano: reinterpretazioni di dati di antiche ricerche di idrocarburi. Memorie della Società Geologica Italiana 12, 227–250.

Iverson RM, Denlinger RP, LaHusen RG, Logan M, (2000) Two-phase debris-flow across 3-D terrain: Model predictions, *in* Wieczorek GF and Naeser ND, eds., Debris-Flow Hazard Mitigation, Mechanics, Prediction, and Assessment: Taipei, Taiwan, 16-18 August 2000: Rotterdam, Balkema, 521-529.

Jenkins SF, Phillips JC, Price R, Feloy K, Baxter PJ, Sri Hadmoko D, de Bélizal E (2015) Developing building-damage scales for lahars: application to Merapi volcano Indonesia. Bulletin of Volcanology 77, 1-17.

https://doi.org/10.5194/egusphere-2023-1302
Preprint. Discussion started: 1 August 2023

Lesti C, Porreca M, Giordano G, Mattei M, Cas R, Wright H, Viramonte J (2011) High temperature emplacement of the Cerro Galán and Toconquis Group ignimbrites (Puna plateau, NW Argentina) determined by TRM analyses. Bulletin of Volcanology 73, 1535-1565.

Lowe DR, Williams SN, Leigh H, Connort CB, Gemmell JB, Stoiber RE (1986) Lahars initiated by the 13 November 1985 eruption of Nevado del Ruiz, Colombia. Nature 324, 51-53.

Lowe DR (1988) Suspended-load fallout rate as an independent variable in the analysis of current structures. Sedimentology 35, 765–776.

Lube G, Cronin S, Manville V, Procter J, Cole S, Freundt A (2012) Energy growth in laharic mass flows. Geology 40, 475-478.

Macedonio G and Pareschi MT (1992) Numerical simulation of some lahars from Mount St. Helens. Journal of Volcanology and Geothermal Research 54, 65-80.

Mariani M and Prato R (1988) I bacini neogenici costieri del margine tirrenico: approccio sismico-stratigrafico. Memorie della Società Geologica Italiana 41, 519-531.

Marotta E., Berrino G., de Vita S., Di Vito M.A., Camacho A.G., 2022. Structural setting of the Ischia resurgent caldera (Southern Tyrrhenian Sea, Italy) by integrated 3D gravity inversion and geological models. In: Marotta, E., D'Auria, L., Zaniboni, F. and Nave, R. (eds) Volcanic Island: from Hazard Assessment to Risk Mitigation. Geological Society, London, Special Publications, 519.

Martí J, Doronzo DM, Pedrazzi D, Colombo F (2019) Topographical controls on small-volume pyroclastic flows. Sedimentology 66, 2297-2317.

McClelland E, Druitt TH (1989) Paleomagnetic estimates of emplacement temperatures of pyroclastic deposits on Santorini, Greece. Bulletin of Volcanology 51, 16-27.

https://doi.org/10.5194/egusphere-2023-1302
Preprint. Discussion started: 1 August 2023

McClelland E (1996) Theory of CRM acquired by grain growth, and its implications for TRM discrimination and paleointensity determination in igneous rocks. Geophysical Journal International 126, 271-280.

Newhall CG and Punongbayan R (Eds.) (1996) Fire and mud: eruptions and lahars of Mount Pinatubo, Philippines. Quezon City: Philippine Institute of Volcanology and Seismology, 1126 pp.

Orsi G, de Vita S, Di Vito MA (1996) The restless, resurgent Campi Flegrei Nested Caldera Italy.: constraints on its evolution and configuration. Journal of Volcanology and Geothermal Research 74, 179-214.

Pareschi MT, Favalli M, Giannini F, Sulpizio R, Zanchetta G, Santacroce R (2000) May 5, 1998, Debris flows in circumvesuvian areas (Southern Italy), insights for hazard assessment. Geology 28, 639-642.

Pareschi MT, Santacroce R, Sulpizio R, Zanchetta G (2002) The volcaniclastic mass flow hazard related to the remobilization of fallout deposits in southern Campania, Italy. Explosive volcanism in subduction zones, Mount Pelée, Martinique, 12-16 May 2002, abstract volume.

Patacca E and Scandone P (2007) Geology of the Southern Apennines. Bollettino della Società Geologica Italiana Special Issue 7, 75-119.

Paterson, GA, Muxworthy AR, Roberts AP, MacNiocaill C (2010). Paleomagnetic determination of emplacement temperatures of pyroclastic deposits: un under-utilized tool. Bulletin of Volcanology, 72, 309-330.

Peccerillo A (2003) Plio-Quaternary magmatism in Italy. Episodes 26, 222-226.

Perrotta A, Scarpati C, Luongo G, Aoyagi M (2006) Burial of Emperor Augustus' villa at Somma Vesuviana (Italy) by post-79 AD Vesuvius eruptions and reworked (lahars and stream flow) deposits. Journal of Volcanology and Geothermal Research 158, 445-466.

https://doi.org/10.5194/egusphere-2023-1302
Preprint. Discussion started: 1 August 2023

Pierson TC (1985) Initiation and flow behavior of the 1980 Pine Creek and Muddy River lahars, Mt. St. Helens, Washington. Geological Society of America Bulletin 96, 1056-1069.

Piochi M, Pappalardo L, Da Astis G (2004) Geo-chemical and isotopical variations within the Campanian Comagmatic Province: implications on magma source composition, Annals of Geophysics 47, 1485-1499.

Pittari A, Cas RAF, Monaghan JJ, Martí J (2007) Instantaneous dynamic pressure effects on the behaviour of lithic boulders in pyroclastic flows: the Abrigo Ignimbrite, Tenerife, Canary Island. Bulletin of Volcanology 69, 265-279.

Porreca M, Mattei M, Mac Niocaill C, Giordano G, McClelland E, Funiciello R (2007) Paleomagnetic evidence for low-temperature emplacement of the phreatomagmatic Peperino Albano ignimbrite (Colli Albani volcano, Central Italy). Bulletin of Volcanology 70, 877-893.

Roche O, Niño Y, Mangeney A, Brand B, Pollock N, Valentine GA (2013) Dynamic pore-pressure variations induce substrate erosion by pyroclastic flows. Geology 41, 1107-1110.

Roche O (2015) Nature and velocity of pyroclastic density currents inferred from models of entrainment of substrate lithic clasts. Earth and Planetary Science Letters 418, 115-125.

Rodolfo KS (2000) The hazard from lahars and jökulhlaups. In: Encyclopedia of Volcanoes: Academic Press, Philadelphia, 973-995.

Rodolfo KS and Arguden AT (1991) Rain-lahar generation and sediment-delivery systems at Mayon Volcano, Philippines: Sedimentation in Volcanic Settings, SEPM Special Publication 45, 71-87.

Rodríguez-Sedano LA, Sarocchi D, Caballero L, Borselli L, Ortiz-Rodríguez AJ, Cerca-Ruiz MF, Moreno-Chávez G, Franco Ramos O (2022) Post-eruptive lahars related to the 1913 eruption in La Lumbre Ravine, Volcán de Colima, Mexico: The influence of ravine morphometry on flow dynamics. Journal of Volcanology and Geothermal Research 421, 107423.

https://doi.org/10.5194/egusphere-2023-1302
Preprint. Discussion started: 1 August 2023

Rolandi G, Barrella AM, Borrelli A (1993) The 1631 eruption of Vesuvius. Journal of Volcanology and Geothermal Research 58, 183-201.

Rolandi G, Munno R, Postiglione I (2004) The A.D. 472 eruption of the Somma volcano. Journal of Volcanology and Geothermal Research 129, 291-319.

Rosi M, Principe C, Vecci R (1993) The 1631 Vesuvius eruption. A reconstruction based on historical and stratigraphical data. Journal of Volcanology and Geothermal Research 58, 151-182.

Rosi M and Santacroce R (1983) The A.D. 472 "Pollena" eruption: volcanological and petrological data for this poorly-known, Plinian-type event at Vesuvius. Journal of Volcanology and Geothermal Research 17, 249-271.

Russell AJ, Knudsen O (1999) An ice-contact rhythmite (turbidite) succession deposited during the November 1996 catastrophic outburst flood (jökulhlaup), Skeidarárjökull, Iceland. Sedimentary Geology 127, 1-10.

Sandri L, de' Michieli Vitturi M, Costa A, Di Vito MA, Rucco I, Doronzo DM, Bisson M, Gianardi R, de Vita S, Sulpizio R, (submitted) Lahar events in the last 2,000 years from Vesuvius eruptions. Part 3: Hazard assessment over the Campanian Plain.

Santacroce R, Cioni R, Marianelli P, Sbrana A, Sulpizio R, Zanchetta G, Donahue DJ, Joron JL (2008) Age and whole rock-glass compositions of proximal pyroclastics from the major explosive eruptions of Somma-Vesuvius: A review as a tool for distal tephrostratigraphy. Journal of Volcanology and Geothermal Research 177, 1-18.

Santacroce R., Sbrana A., Andronico D., Cioni R., Di Vito M., Marianelli P., Sulpizio R., Zanchetta G., Arrighi S., Benvenuti E., Gurioli L., Leoni F.M., Luperini W., 2003. Carta Geologica del Vesuvio in scala 1:15.000, Santacroce R., Sbrana A., eds. Cartografia derivata dai rilievi geologici in scala 1:10.000 Regione Campania e dai rilievi in scala 1:25.000 del Progetto CARG., S.EL.C.A., Firenze.

https://doi.org/10.5194/egusphere-2023-1302
Preprint. Discussion started: 1 August 2023

Santangelo N, Romano P, Ascione A, Russo Ermolli E (2017) Quaternary evolution of the Southern Apennines coastal plains: A review. Geologica Carpathica 68, 43-56.

Scott KM (1989) Magnitude and frequency of lahars and lahar-runout flows in the Toutle-Cowlitz River System. U. S. Geological Survey Professional Paper 1447-B, 1–33.

Scott KM, Vallance JW, Pringle PT (1995) Sedimentology, behavior, and hazard of debris flows at Mount Rainer, Washington. U. S. Geological Survey Professional Paper 1547, 1-56.

Scott KM, Macìas JL, Naranjo JA, Rodriguez S, McGeehin JP (2001) Catastrophic debris flows transformed from landslide in volcanic terrains: mobility, hazard assessment and mitigation strategies. US Geol Surv Prof Pap. 1630, 1-59.

Sheridan MF, Bonnard C, Carrero C, Siebe C, Strauch W, Navarro M, Calero JC, Trujillo NB (1999) Report of the 30 October 1998 rock fall/avalanche and breakout flow of Casita Volcano, Nicaragua, triggered by Hurracane Mitch. Landslide News 12, 2-4.

Siebe C, Schaaf P, Urrutia-Fucugauchi J (1999) Mammoth bones embedded in a late Pleistocene lahar from Popocatépetl volcano, near Tocuila, central Mexico. Geological Society of America Bulletin 111, 1550-1567.

Spence RJS, Zuccaro G, Petrazzuoli S, Baxter PJ (2004) Resistance of buildings to pyroclastic flows: analytical and experimental studies and their application to Vesuvius. Natural Hazards Review 5, 48-59.

Sulpizio R, Mele D, Dellino P, La Volpe L (2005) A complex, Subplinian-type eruption from low-viscosity, phonolitic to tephri-phonolitic magma: the AD 472 (Pollena) eruption of Somma-Vesuvius, Italy. Bulletin of Volcanology 67, 743-767.

https://doi.org/10.5194/egusphere-2023-1302
Preprint. Discussion started: 1 August 2023

Sulpizio R, Zanchetta G, Demi F, Di Vito MA, Pareschi MT, Santacroce R (2006) The Holocene syneruptive volcaniclastic debris flows in the Vesuvian area: Geological data as a guide for hazard assessment. Geological Society of America Special Paper 402, 203-221.

Tema E, Zanella E, Pavón-Carrasco FJ, Kondopoulo D, Pavlides S (2015) Palaeomagnetic analysis on pottery as indicator for the pyroclastic flows deposit temperature: New data and statistical interpretation from the Minoan eruption of Santorini, Greece. Geophysical International Journal 203, 33-47.

Thouret JC, Arapa E, Charbonnier S, Guerrero A, Kelfoun K, Cordoba G, Rodriguez D, Santoni O (2022) Modeling tephra fall and sediment-water flows to assess their impact on a vulnerable building stock in the City of Arequipa, Peru. Frontiers in Earth Science 10, 865989.

Toyos G, Gunasekera R, Zanchetta G, Oppenheimer C, Sulpizio R, Favalli M, Pareschi MT (2008) GIS-assisted modelling for debris flow hazard assessment based on the events of May 1998 in the area of Sarno, Southern Italy: II. Velocity and dynamic pressure. Earth Surface Processes and Landforms 33, 1693-1708.

Vallance JW and Iverson R (2015) Lahars and their deposits. In: Sigurdsson, H., Houghton, B.F., McNutt, S.R., Rymer, H., Stix, J. (Eds.), Encyclopedia of Volcanoes. Academic Press, London, 649-664.

Vallance JW and Scott KM (1997) The Osceola mudflow from Mount Rainer: Sedimentology and hazards implications of a huge clay-rich debris flow. Geological Society of America Bulletin 109, 143-163.

Vitale S and Ciarcia S (2018) Tectono-stratigraphic setting of the Campania region (southern Italy), Journal of Maps 14, 9-21.

Voight B (1990) The 1985 Nevado del Ruiz volcano catastrophe: anatomy and retrospection. Journal of Volcanology and Geothermal Research 42, 151-188.

https://doi.org/10.5194/egusphere-2023-1302
Preprint. Discussion started: 1 August 2023

Waitt RB Jr, TC Pierson TC, MacLeod NS, Janda RJ, Voight B, Holcomb RT (1983) Eruption-triggered avalanche, flood, and lahar at Mount St. Helens - Effects of winter snowpack. Science 221, 1394-1397.

Whipple KX, Hancock GS, Anderson RS (2000) River incision into bedrock: Mechanics and relative efficacy of plucking, abrasion, and cavitation. Geological Society of America Bulletin 112, 490-503.

White S, García-Ruiz JM, Martí-Bono C, Valero B, Errea MP, Gómez-Villar A (1997) The 1996 Biescas campsite disaster in the Central Spanish Pyrenees and its spatial and temporal context. Hydrological Processes 11, 1797-1812.

Zanchetta G, Sulpizio R, Di Vito MA (2004b). The role of volcanic activity and climate in alluvial fan growth at volcanic areas: an example from southern Campania (Italy). Sedimentary Geology 168, 249-280.

Zanchetta G, Sulpizio R, Pareschi MT, Leoni FM, Santacroce R (2004a) Characteristics of May 5-6, 1998 volcaniclastic debris flows in the Sarno area (Campania, southern Italy): relationships to structural damage and hazard zonation. Journal of Volcanology and Geothermal Research 133, 377-393.

Zanella E, Gurioli L, Pareschi MT, Lanza R (2007). Influences of urban fabric on pyroclastic density currents at Pompeii (Italy): 2. Temperature of the deposits and hazard implications. Journal of Geophysical Research 112, B05214.

Zanella E, Gurioli L, Lanza R, Sulpizio R, Bontempi M (2008). Deposition temperature of the AD 472 Pollena pyroclastic density current deposits, Somma-Vesuvius, Italy. Bulletin of Volcanology 70, 1237-1248.

Zanella E, Sulpizio R, Gurioli L, Lanza R (2015). Temperatures of the pyroclastic density currents deposits emplaced in the last 22 kyr at Somma-Vesuvius (Italy). Geological Society, London, Special

https://doi.org/10.5194/egusphere-2023-1302
Preprint. Discussion started: 1 August 2023

Publication, The Use of Palaeomagnetism and Rock Magnetism to Understand Volcanic Processes 396.

Zuccaro G, De Gregorio D (2013) Time and space dependency in impact damage evaluation of a sub-Plinian eruption at Mount Vesuvius. Natural Hazards 68, 1399-1423.